



## Original paper

### Assessing Groundwater Potential and Recharge Zones Using Integrated Remote Sensing and GIS Techniques in Bannu Basin, Pakistan

Muhammad Jamal Nasir<sup>1</sup> , Abdur Raziq<sup>2</sup> , Jawad Ur Rahman<sup>1</sup>,  
Ayad M. Fadhil Al-Quraishi<sup>3\*</sup> 

<sup>1</sup>Department of Geography, University of Peshawar, Peshawar 25120, Pakistan

<sup>2</sup>Department of Geography, Islamia College Peshawar, Peshawar 25120, Pakistan

<sup>3</sup>Petroleum and Mining Engineering Department, Tishk International University, Erbil 44001, Iraq

\*Corresponding author: [ayad.alquraishi@gmail.com](mailto:ayad.alquraishi@gmail.com), ORCID: 0000-0001-7732-129X

## ARTICLE INFO

### Article history:

Received: 05 May, 2025

Revised: 25 October, 2025

Accepted: 25 November, 2025

## ABSTRACT

Surface water has usually served as a reliable source for meeting the water needs of humans. However, rapid urbanization and industrialization have significantly altered water dynamics. This study examined groundwater potential and its recharge sites in the Bannu Basin, Pakistan, using geospatial technologies. The study applied multi-influencing factors and weighted overlay analysis techniques with eight influencing parameters, including land use/land cover, soil, drainage and lineament density, topography, rainfall, geology, and runoff potential. To achieve this, Sentinel-2 (2022) was used to create a land use/land cover layer, and runoff potential was computed using land use/land cover, rainfall, and soil data. The resulting layers were categorized into four classes: excellent, good, moderate, and poor. Overall, the analysis shows that significant groundwater potential justifies 47.92% of the area, which covers the central part, excellent as 4.56% covering a very minor area of 50.14 km<sup>2</sup>, moderate as 38.96% covering the northeastern and southern parts, while poor accounts for 8.57% of the total study area. As a result, a major part of the area has moderate to good groundwater recharge potential, with a small portion (1.15%) having excellent groundwater potential, whereas poor groundwater recharge potential prevails in 340.33 km<sup>2</sup> (7.81%). The study results were confirmed using field data and a groundwater potential map by overlay analysis with the real groundwater table, showing that lower water tables match poor and higher tables with excellent potential zones. This study will help in sustainable groundwater resource management and planning in similar regions.

**Keywords:** Surface water, multi-influencing factors, runoff potential, weighted overlay analysis, geospatial environment

## INTRODUCTION

Water, particularly freshwater, is considered the basis of human life. Nevertheless, it comprises less than 3% of the world's water resources. As a natural supply to the entire earth ecosystem, it is one of the most significant renewable resources used for drinking, agricultural purposes, and many other living purposes (Gaikwad et al., 2018; Adimalla et al., 2018). On a global scale, 96% of water sources account for almost 332.5

million cubic meters of saline water. In contrast, groundwater is preferable to surface water because it is pure and safe before processing (Akudo et al., 2010). In Pakistan, groundwater is a significant source for urban and rural areas, which is mainly used for manufacturing and agricultural needs. In addition, one-third of groundwater resources are used for irrigation (Qureshi et al., 2015). Consequently, despite

the presence of large rivers and streams, surface water in Pakistan is scarce (Sato et al., 2019; Trung et al., 2020).

Owing to the impact of global climate change, people must control their requirements for ground and surface water and monitor global groundwater for the durable utilization of natural resources (Oh et al., 2011). Owing to expanding economies and rapid population growth, the global demand for fresh water is growing significantly. Moreover, with rapid urbanization, the need for freshwater in urban areas has become a pressing challenge (Rajasekhar et al., 2020; Fagbohum, 2018). Pakistan is an agricultural country, and groundwater is its primary source of fresh water, which is recorded at 66 million acres annually (Hassan et al., 2016). Hence, groundwater demand has become a critical parameter in water management systems (Senanayake et al., 2016). To achieve this, an analysis of groundwater resources is significant for eco-friendly management, and the selection of recharge sites is necessary for current water resource management.

Remote sensing (RS) and Geographic Information Systems (GIS) have been extensively used to manage different natural resources, including water resources (Dar et al., 2010; Krishna et al., 2011). Particularly for groundwater, geospatial researchers are actively promoting the introduction of an integrative approach to RS, GIS, multiple influencing factors (MIF), and overlay analysis to find optimal recharge sites (Khan et al., 2021; Faheem et al., 2023). Groundwater is significantly impacted by various parameters, including geology, geomorphology, climate, drainage network, aquifer properties, and human activities (Deshmukh, 2011; Kalpana and Elango, 2013).

The MIF method is widely used to validate the impact of single parameters on the hydrological arrangement of an area (Magesh et al., 2012; Nasir et al., 2018; 2021; Etikala et al., 2019). For instance, in integrating GIS, Abdullah et al. (2022) and used the MIF approach to assess suitable sites for rainwater harvesting (RWH) in Khyber Pakhtunkhwa (KP).

Moreover, the application of geospatial data has been optimally utilized in the identification and

delineation of potential groundwater areas and sites, as well as groundwater zones (Saravanan et al., 2022; Vasanthavigar et al., 2013; Preeja et al., 2011; Murugesan et al., 2012; Mukherjee et al., 2012; Thapa et al., 2017; Yadav et al., 2023). Additionally, RS data, together with GIS analysis, can precisely detect areas with potential and need for RWH structures with a holistic approach to community participation in RWH projects, hence leading to maintainable agricultural practices and better water management techniques.

Many researchers have employed an additional weighted overlay method (WOM) with RS and GIS techniques to identify potential groundwater zones (Sohail et al., 2019; Datta et al., 2020; Akudo et al., 2024; Alam et al., 2022; Khan et al., 2022; Afzal et al., 2023; Ahmad et al., 2024). With the application of fuzzy logic and related models, similar studies have efficiently monitored the RWH-based potential of sites and focused areas. Moreover, related studies using analytical hierarchy process (AHP) and MIF approaches (Jebaraj and Rajagopal, 2024; Multaniya et al., 2024; Shinde et al., 2024) have found MIF analysis to be the most valid, cost-effective, and attainable approach.

Related to groundwater potential (GWP) and recharge site identification, the present study focused on the Bannu Basin in KP province, applying RS and GIS, weighted overlay, and integrating eight MIF influencing factors. Covering an area of 10,030 km<sup>2</sup> and an alluvial plain of 4,200 km<sup>2</sup>, the focused study basin is situated on the right bank of the Indus River. It is divided by the Marwat and Shinghar ranges. Due to the population increase, scant rainfall, and high demand for agriculture and industry, the region is critical for groundwater restoration. However, according to previous studies on RWH, particularly for the Bannu Basin, no existing studies have been found on the RWH issue. This study aimed to assess the GWP and identify suitable areas for groundwater recharge and intrusion in the Bannu Basin, Pakistan. This was achieved by employing integrated RS and GIS, MIF, and WOMs to create a lead map of groundwater resources for sustainable water resource management, monitoring, and guidance.

## MATERIALS

### Study Area

This study was conducted in the Bannu Basin, Pakistan (Fig. 1), which contains a share of Laki Marwat, Karak, and the district Bannu. Geographically, the Bannu Basin is situated between  $32^{\circ}20'$  -  $33^{\circ}05'$  N latitude and  $70^{\circ}20'$  -  $71^{\circ}10'$  E longitude, enclosed by the Bannu District to the north, South Waziristan and Tank to the west, Karak to the east, and Lakki Marwat to the south. The area cover is  $4360.31\text{ km}^2$  and has a population of 3,092,078. Geographically, the Bannu Basin was initially part of the Indo-Gangetic headland basin until approximately 500,000 years ago, when the upthrust of the Bhittani and Marwat series shifted it. The Kohat encloses the basin, the Waziristan-Suleiman ranges to the north, the Bhittani series to the west, the Marwat series to the south, and the Shinghar series to the east.

The Gambila River enters from the southwest, flows southeast, and bends eastward, eventually merging with the Kurram River. In addition

to perennial streams, impermanent streams transmit runoff to the Gambila and Kurram rivers after rainstorms. The elevation of the area falls from 826 m in the west to 211 m in the east. The climate is characterized by hot summers (average high  $35.3^{\circ}\text{C}$ , low  $27.3^{\circ}\text{C}$ ) and mild winters (high  $13.1^{\circ}\text{C}$ , low  $4.8^{\circ}\text{C}$ ), with an average annual rainfall of 120.66 mm (4.75 inches) and 133.34 days of precipitation (Rahman et al., 2021). Agriculture, which primarily relies on groundwater for irrigation, is the backbone of the local economy. Key crops include watermelons, wheat, and chickpea. However, the unsustainable use of groundwater resources for agricultural, residential, and commercial purposes has led to groundwater depletion and deteriorating water quality (Jalil et al., 2020).

### Data Collection

Primary and ancillary data were used to achieve the study's objectives. All influencing parameters (IP) and selected variables were

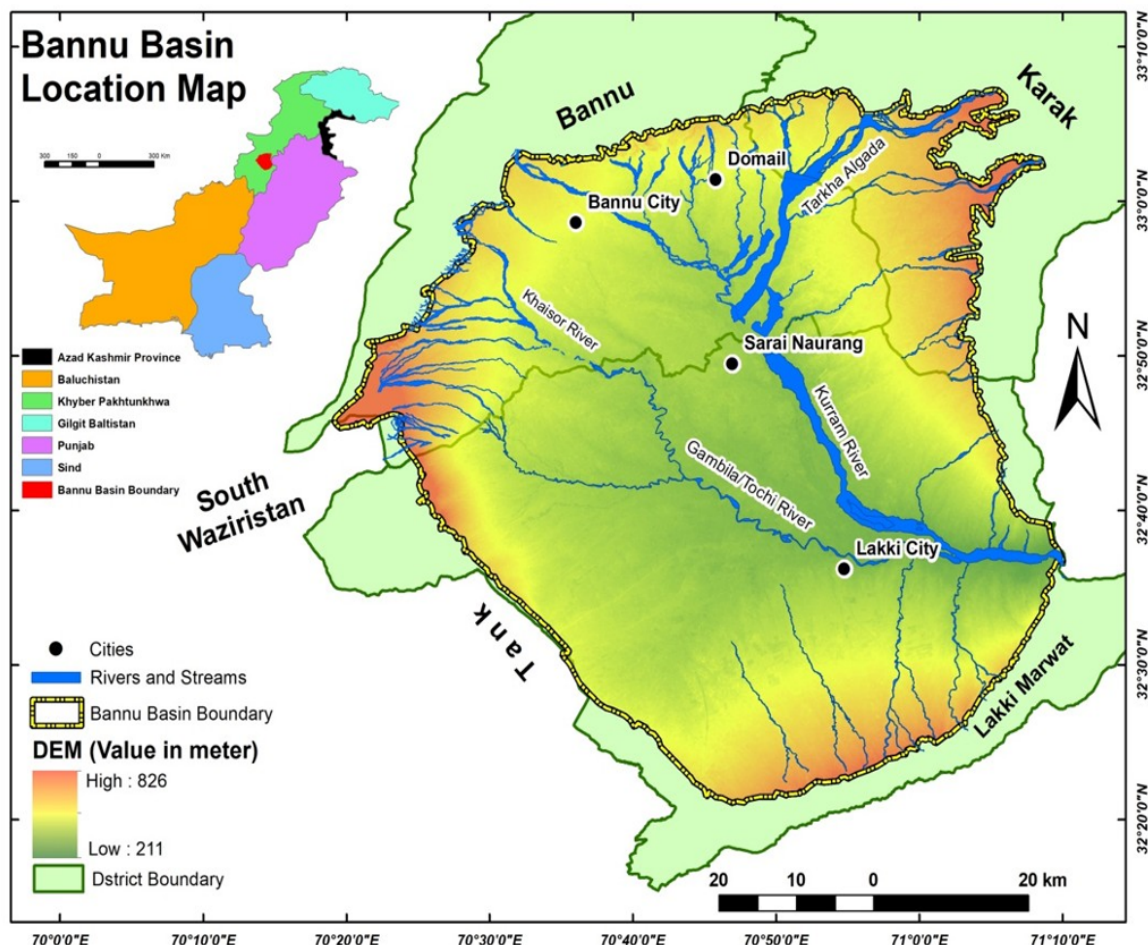


Fig. 1. Location map of the study area

acquired from various sources. The primary data consisted of well locations and groundwater table (GWT) levels. The locations of the tube wells were determined in the field using a global positioning system (GPS). The XY coordinates of the tube wells were saved in the GPS as waypoints. The GWT level was achieved using a wire, with a metal nut at its end. Slight surface turbulence was observed upon interaction with water, and minor tension loss in the rope was indicated when the weight touched the bottom. The total depth was calculated by measuring the length of the rope positioned at that point. Some data were supplemented by reports from local residents regarding the water levels in their wells. GWT data were used to confirm the GWP analysis output. Secondary data, including the base map for the Bannu Basin boundary, were obtained from a survey of Pakistan and district census reports. The map was used to extract the area of concentration from satellite images, geological data, and IPs.

### Land Use/Land Cover (LULC)

LULC is a critical factor in groundwater recharge. Satellite imagery of Sentinel-2 with a 10-m resolution in 2022 was acquired from the USGS website ([USGS, 2022](#)). The acquired images were used to produce LULC maps using the ArcGIS software spatial analysis tool and employing Maximum Likelihood supervised classification. The images were classified into six LULC classes: built-up areas, rangeland, barren land, cultivated land, vegetation, and water. Each LULC category was assigned a score value based on its efficiency in groundwater recharge potential using MIF techniques ([Nasir et al., 2021](#)). Furthermore, LULC data were used to examine and define the groundwater recharge potential area by combining rainfall data and the hydrological soil group (HSG).

### Soil Data

Soil penetrability, which is influenced by numerous factors, is vital for defining potential groundwater regions. Soil data were obtained from the Department of Soil and Water Conservation and the US Agriculture Department, with HSG data. These data were used to measure the runoff potential of the

research area in integration with LULC. The HSG data were recategorized based on porosity, permeability, and groundwater recharge efficiency. Soil category distribution and groups were examined in relation to recharge potential and porosity, with weights and values assigned to reflect the variable impacts on groundwater recharge ([Nasir et al., 2021; Mandal et al., 2021](#)).

### Topographic Data

Elevation, slope, and drainage density (DD) were determined using ASTERDEM 2.0, with 17-m accuracy and 30-m resolution, downloaded from the website ([Tachikawa et al., 2011](#)). The digital elevation model (DEM) was examined using the hydro-tool ArcMap 10.8. The following steps were adopted to extract the drainage network: 1) Manipulation of DEM to create a DEM free from sinks and fills. 2) Flow direction and accumulation grids. 3) Stream Definition and Segmentation. 4) Raster-to-vector conversion of the stream-to-feature command. 5) Stream density creation using a line-density tool.

### Rainfall Data

Rainfall, as the main source of aquifer recharge, plays a vital role in groundwater replenishment. To examine strength charges and calculate weight, the research area was classified into rainfall classes using an equal interval approach in ArcGIS. Temperature and rainfall data for 2018-2022 were acquired from weather stations in Parachinar, D.I. Khan, and Bannu. An interpolation method was used to assess changes in GWP ([Nasir et al., 2018, 2021](#)). Global weather and climate data were acquired from WorldClim 1 to validate the rainfall data.

### Geological Data

Groundwater availability is influenced by the geological composition and rock types present. While some rocks resist water infiltration, thereby affecting recharge rates, most rocks absorb and retain water for extended periods, creating a buffer zone that supports recharge. The geological map was derived from the published map of Khyber Pakhtunkhwa by M. Asif Khan and M.P Sealer. This map was geo-

referenced and digitized using ArcGIS, and rocks were categorized based on their potential for groundwater recharge and their minor and major influencing factors. The classification process involved assigning values and weights to the different rock classes (Nasir et al., 2018, 2021).

## Runoff Potentiality

In water management, runoff is a crucial hydrodynamic element influenced by factors such as infiltration, inherent characteristics, and precipitation (Adham et al., 2014). Variables related to rainfall, including intensity, duration, and distribution, play a significant role in determining both the volume and timing of runoff, with variations observed across different months and seasons (Tailor and Shrimali, 2016). Understanding runoff is essential for managing groundwater, planning hydrological activities, and monitoring the environment. Various methods have been employed to assess runoff potential, such as the geomorphological instantons unit hydrograph

(GIUH), University of British Columbia watershed Model (UBCWM), Artificial Neural Network (ANN), Rational and Green-Ampt approaches (Tailor and Shrimali, 2016), and the soil conservation service-curve number (SCS-CN) approach (Khan et al., 2022). The curve number (CN) approach is particularly renowned for its straightforwardness, effectiveness, and reliability (Ebrahimian, 2012).

## METHODS

The growing need for groundwater, driven by reduced surface water for agricultural, industrial, and drinking water, has made the identification of viable groundwater zones critical. Rapid urbanization, irregular water distribution, climate variability, and rising temperatures have exacerbated surface water scarcity. Therefore, highlighting the main groundwater zones is crucial. This study examined the data needed to understand aquifer systems and the tendency of groundwater resource growth. The objective of this study was to assess and define GWP and recharge zones in the Bannu Basin,

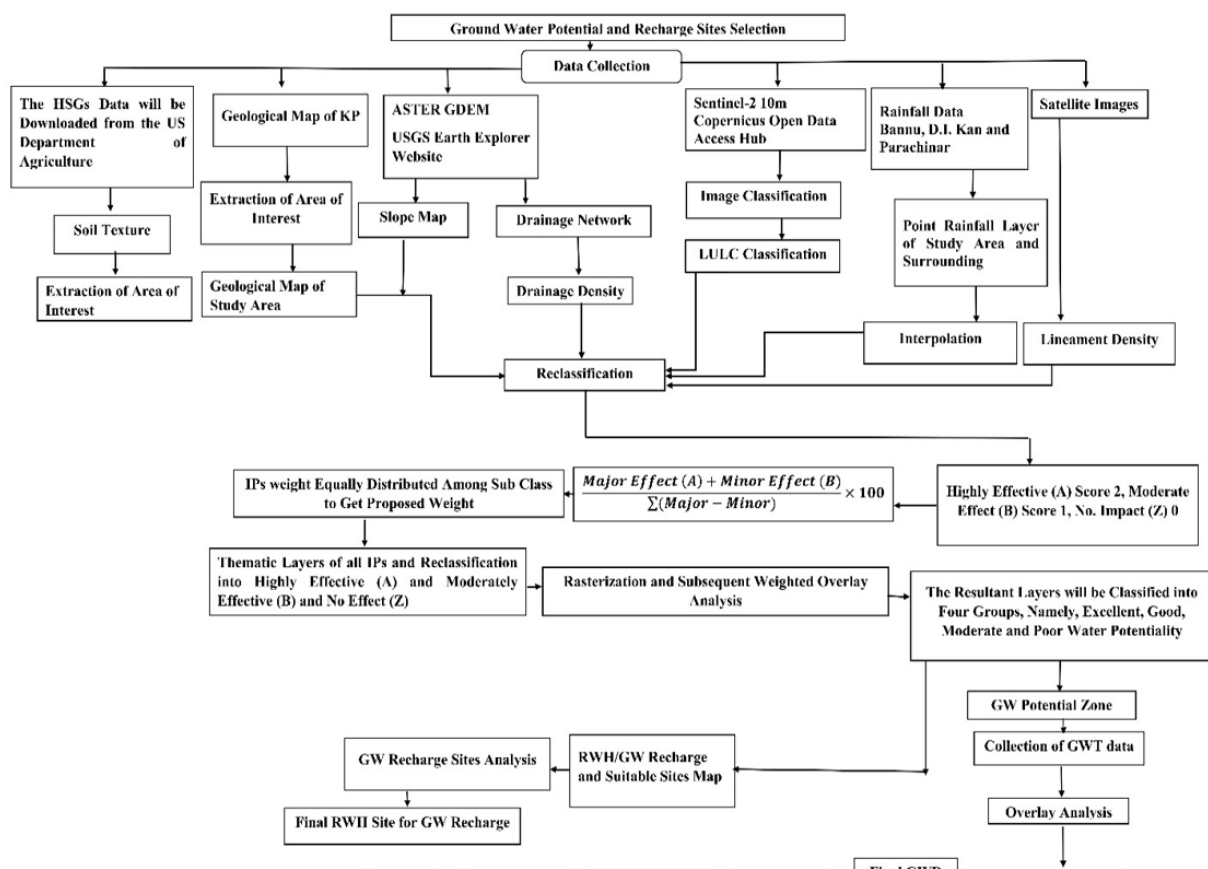


Fig. 2. Flow Chart of the research methodology

Khyber Pakhtunkhwa. Fig. 2 shows the adopted methodology.

### Multi-Influencing Factors (MIF)

The MIF approach is widely recognized as the primary method for assessing GWP and was chosen to achieve the study objectives (Thapa et al., 2017; Nasir et al., 2018; Mandal et al., 2021; Zghibi et al., 2020). The initial step in the MIF approach is to assign values to the subcomponents of the nominated IP. Each subclass was evaluated for its effectiveness in groundwater aquifer recharge. Subcomponents extremely effective in recharge “A” were assigned value 2, moderately effective “B” were given value 1, and no impact (Z) 0. The total scores (A+B) of the highly effective (A) and moderately effective (B) subcomponents were combined to calculate the relative effect. The relative weight of each IP was determined by the formula below in Equation (1).

$$\text{Proposed weight} = \frac{\text{Major Effect (A)} + \text{Minor Effect (B)}}{\sum (\text{Major Effect (A)} + \text{Minor effect (B)})} \times 100 \quad (1)$$

Subsequently, weights were assigned to the nominated parameter subclasses, with each IP weight consistently distributed among its subcomponents (Gumma and Pavelic, 2013). The next step involved rasterizing and regrouping all the IP layers, integrating both score and weight values, and utilizing ArcMap 10.8 for weighted overlay analysis. The subsequent output layer was classified into four classes: excellent, good, moderate, and poor GWP, after integrating all the IP layers. A similar method was used by Faeem et al. (2023) to find groundwater recharge potential sites without runoff potential, which was also assessed as an IP. Runoff potential was considered using LULC and hydrological soil data.

### Weighted Overlay Analysis

#### Parameter Weighting and Standardization

The method for assigning weight values to select parameter subclasses in the GWP assessment of the Bannu Basin involves several key steps. The designated parameter layers were regrouped into five subclasses based on their efficiency in groundwater recharge, excluding LULC and geology, which were grouped into six classes,

as shown in column B of Table 1. The weight value for every subclass was then assigned based on its efficiency in terms of GWP.

The proposed sum effects of the parameter are calculated by Equation (2)

$$\sum (A + B) \quad (2)$$

Where A+B is the total of the parameters of the subclass's comparative effect score and the total of columns D and E in Table 1. We followed the method proposed by Zghibi et al. (2020) to calculate each IP in Equation (1).

Where A+B is the total relative effect score of the parameter subclasses,  $\sum (A+B)$  is the total weight score of all the parameter subclasses, and columns D and E are shown in Table 1, which illustrates the weight score assigned to different subclasses of all the variable parameters selected for analysis. Table 2 illustrates the weighted parameters of each class assigned to the maps.

### Categorization of Groundwater Potential (GWP) Zones

The weighted overlay analysis followed a designated process as described below. The initial step involves assigning weights to the subclass parameters, with the proposed weights from Equation (3) spread equally (Gumma and Pavelic, 2013). The weight values for each subclass are listed in Table 1. The 2<sup>nd</sup> step involved rasterizing every parameter layer and regrouping it with the allocated weights using the ArcMap spatial analysis tool. The 3<sup>rd</sup> step contains totaling all regrouped parameter layers in the ArcMap weighted overlay analysis. Influence weights were assigned based on the literature, expert opinion, and parameter efficiency: rainfall and LULC received 20%, soil and geology 15%, and slope, drainage, and lineament density 10% (Thapa et al., 2017; Nasir et al., 2018; Shao et al., 2020). The output GWP layers were then regrouped into four classes: excellent, good, moderate, and poor, and the area of each zone was computed.

## RESULTS AND DISCUSSION

### MIF

#### Drainage Density (DD)

DD signifies a drainage density network that represents the movement of streams

**Table. 1.** Weight scores were assigned to various subclasses of variable parameters selected for the analysis

A	B	C	D	E	F	G
IP	Sub categories of the IP	Qualitative Ranking	Major effect (A)	Minor Effect (B)	relative sum of Effects (A+B)	Proposed weightage of each IP (A+B)/Σ(A+B)x100
DD m/km <sup>2</sup>	0.55 - 0.9	Very High	2	-	6	13.6
	0.38 - 0.55	High	2	-		
	0.23 - 0.37	Moderate	-	1		
	0.082 - 0.22	Low	-	1		
	0 - 0.081	Very Low	-	-		
LD km/km <sup>2</sup>	0.62 - 0.77	Very High	2	-	6	13.6
	0.47 - 0.61	High	2	-		
	0.32 - 0.46	Moderate	-	1		
	0.16 - 0.31	Low	-	1		
	0 - 0.15	Very Low	-	-		
LULC	Water	Very High	2	-	8	18.18
	Cultivated land	Very High	2	-		
	Vegetation	High	2	-		
	Rangeland	Moderate	-	1		
	Built-up Area	Low	-	1		
	Barren land	Very Low	-	-		
Geology	Water	Very High	2	-	8	18.18
	Alluvium, Sandstone	Very High	2	-		
	Conglomerate, Mudstone	High	2	-		
	Calcareous shale, Limestone	Moderate	-	1		
	Red-Clastic Sandstone, Shale	Moderate	-	1		
	Dolomite, Quartzite	Low	-	-		
Soil	Lithosols	Very High	2	-	4	9.09
	Haplic Xerosols	High	2	-		
Rainfall in mm.	429 - 457	Very High	2	-	6	13.63
	399 - 428	High	2	-		
	370 - 398	Moderate	-	1		
	340 - 369	Low	-	1		
	310- 339	Very Low	-	-		
Topography (Slope) In Degrees.	0 - 8	Very High	2	-	6	13.63
	9 - 16	High	2	-		
	17 - 24	Moderate	-	1		
	24 - 32	Low	-	1		
	32 - 35.2	Very Low	-	-		
			$\Sigma A=32$	$\Sigma B=12$	$\Sigma A + B = 44$	$\Sigma 100$

**Table 2.** Thematic layers and scores were assigned to the maps

IP	Sub categories of the IP	Qualitative Ranking	Proposed weightage each IP	Quantitative Ranking	Weightage
DD m/km <sup>2</sup>	0 - 0.081	Very High	13	13	10
	0.082 - 0.22	High		10	
	0.23 - 0.37	Moderate		7	
	0.38 - 0.55	Low		4	
	0.55 - 0.9	Very Low		1	
LD km/km <sup>2</sup>	0.62 - 0.77	Very High	13	13	10
	0.47 - 0.61	High		10	
	0.32 - 0.46	Moderate		7	
	0.16 - 0.31	Low		4	
	0 - 0.15	Very Low		1	
LULC	Water	Very High	25	18	20
	Cultivated land	Very High		15	
	Vegetation	High		12	
	Rangeland	Moderate		8	
	Built-up Area	Low		4	
	Barren land	Very Low		1	
Geology	Water	Very High	18	18	15
	Alluvium, Sandstone	Very High		15	
	Conglomerate, Mudstone	High		12	
	Calcareous shale, Limestone	Moderate		8	
	Red-Clastic Sandstone, Shale	Moderate		4	
	Dolomite, Quartzite	Low		1	
Soil	Lithosols	Very High		7	15
	Haplic Xerosols	High		3	
Rainfall in mm	429 - 457	Very High	18	18	20
	399 - 428	High		13	
	370 - 398	Moderate		9	
	340 - 369	Low		5	
	310 - 339	Very Low		1	
Topography (Slope) In Degrees	0 - 8	Very High	13	13	10
	9 - 16	High		10	
	17 - 24	Moderate		7	
	24 - 32	Low		4	
	32 - 35.2	Very Low		1	
				$\Sigma 100$	

and rivers. DD is defined as the total stream distance per unit of drainage area. It is stated in-stream distance per  $\text{km}^2$  (Strahler, 1964). It is widely used in geography, hydrology, and environmental science to represent sites and hydrological phenomena. DD was described using the following Equation (3):

$$DD = \frac{L}{A} \quad (3)$$

Where  $L$  -is the length of the total channel and  $A$  -is the total area. High  $DD$  indicates a dense stream network and higher surface runoff, which are characteristically linked with low permeability and partial infiltration, thereby reflecting a lower GWP. In contrast, a low  $DD$  indicates fewer streams and better infiltration capacity, which is usually linked to a higher GWP due to an increased recharge potential (Strahler, 1964; Mahmoud and Alazba, 2016).

**Table 3.** The DD of the area in  $\text{km}^2$

DD Classes	Qualitative Ranking	Area in $\text{km}^2$	Percentage
0-0.081	Very Low	1879.95	43
0.82 - 0.22	Low	657.174	15
0.23 - 0.37	Moderate	865.1674	20
0.38 - 0.55	High	647.3763	15
0.56 - 0.9	Very High	310.653	7
Total		4360	100

In this study, the  $DD$  area was categorized into five classes: very low (0-0.081), low (0.082-0.22), moderate (0.023-0.37), high (0.38-0.55), and very high ( $> 0.56$ ). Fig. 3 shows the spatial distribution of these classes. The area enclosed by each class is as follows: high ( $647.3763 \text{ km}^2$ ), very high ( $310.653 \text{ km}^2$ ), moderate ( $865.1674 \text{ km}^2$ ),

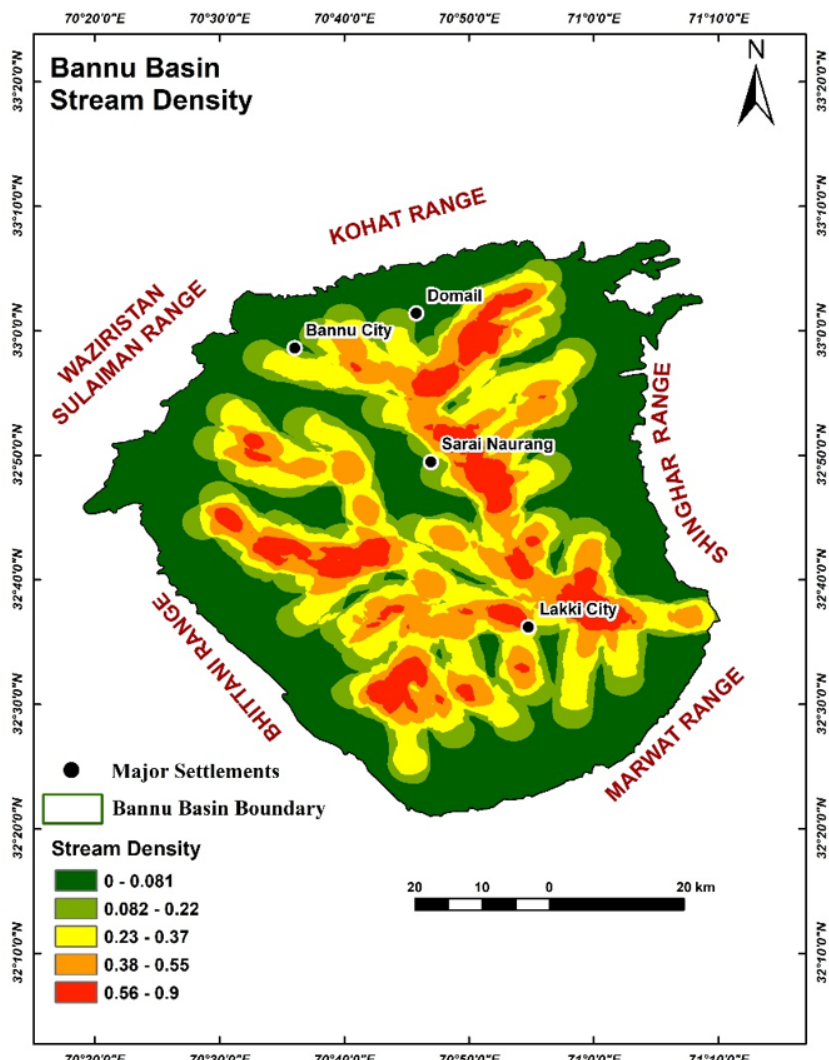


**Fig. 3.** DD map showing classification

km<sup>2</sup>), very low (1879.95 km<sup>2</sup>), and low (657.174 km<sup>2</sup>). A higher value was allocated to the very low *DD* class, as it showed greater infiltration capacity and less surface runoff (Nasir et al., 2018). Table 3 shows the area and percentage of each *DD* category in the study area.

### Lineament Density (LD)

LD is a geological and geomorphological parameter that counts the density of linear features, called lineaments, such as fractures, joints, faults, and related geological structures. Evaluating LD provides insight into a region's tectonic, structural, and geological features, as well as the permeation potential of rocks and soil. LD was calculated using Equation (4).

$$\text{Lineament Density} = \frac{\text{Total Length of Lineament}}{\text{Total Basin Area}} \quad (4)$$

Higher LD values indicate greater sensitivity to linear features, a multifaceted geological history, and improved soil and rock infiltration, which are essential for GWP. According to (O' Leary et al., 1976; Nag and Kundu, 2018), LD can be found beneath fractures and creaks that may assist groundwater basins. RS methods, such as aerial photography and satellite imagery, are typically applied to map lineaments in GIS. In the present study, LD for the Bannu basin was categorized into five classes: very high (0.62-0.77), high (0.47-0.61), medium (0.32-0.46), very low (0-0.15), and low (0.16-0.31). Table 4 illustrates the content for each class: very high (25.13 km<sup>2</sup>, 1%), high (245.68 km<sup>2</sup>, 6%), medium (882.18 km<sup>2</sup>, 20%), very low (1475.86 km<sup>2</sup>, 34%), and low (1730.65 km<sup>2</sup>, 40%). Fig. 4 shows the spatial distribution of the LD classes. According to the GWP, LD in high- and very-

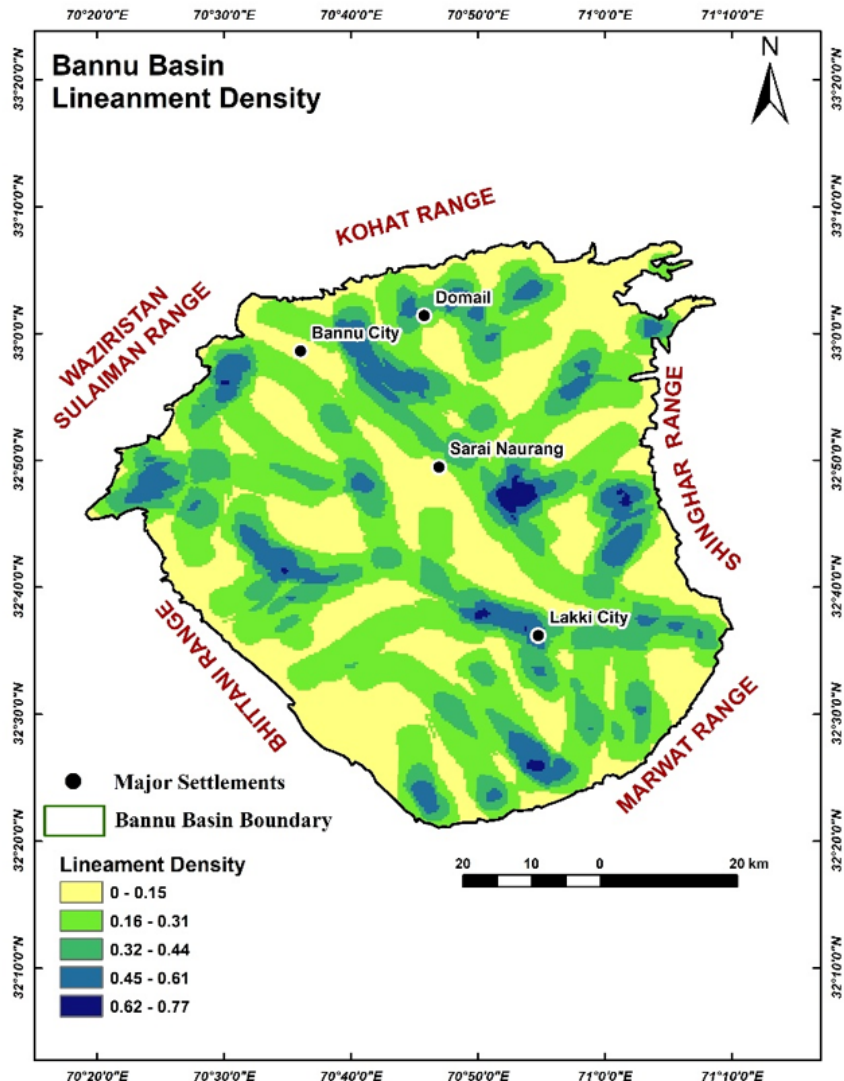


Fig. 4. LD map showing class intervals

**Table 4.** The LD in km<sup>2</sup>

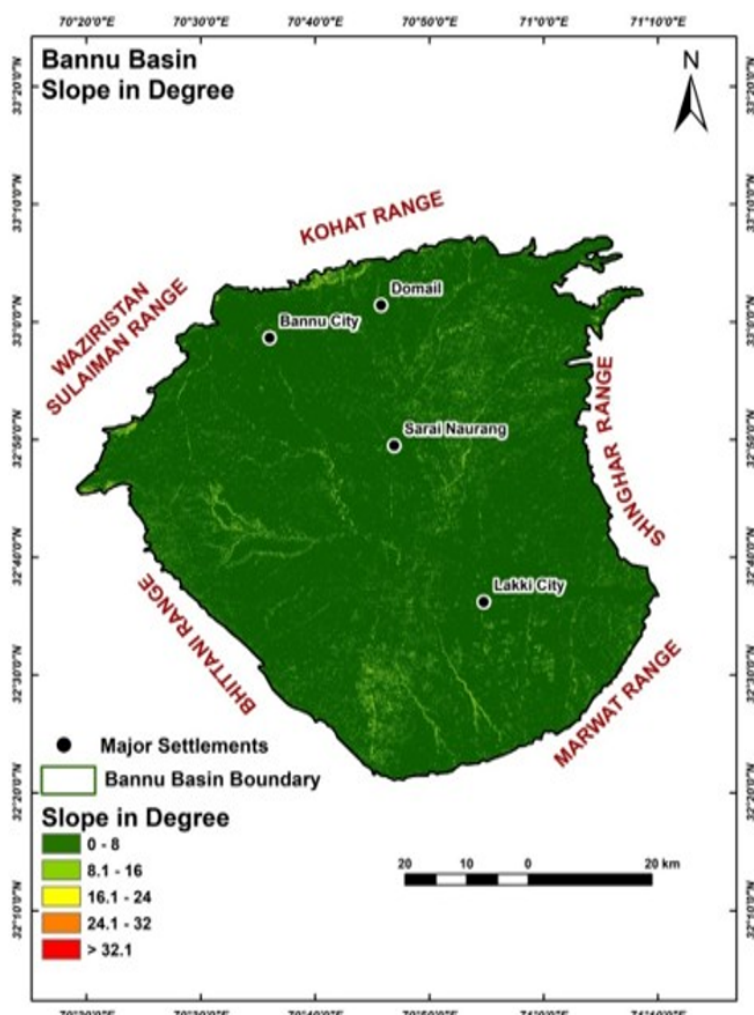
LD Classes	Qualitative Ranking	Area in km <sup>2</sup>	%
0-0.15	Very Low	1475.86	34
0.16 - 0.31	Low	1730.65	40
0.32 - 0.46	Moderate	882.18	20
0.47 - 0.61	High	245.68	6
0.62 - 0.77	Very High	25.13	1
Total		4360	100

high areas was assigned a value of 2, covering 270.82 km<sup>2</sup> (7% of the total area). Nasir et al. (2018) suggested that areas with very high LD were assigned higher values, while areas with lower LD were assigned lower scores, covering 145.93 km<sup>2</sup>, 34%. The results indicated that a major portion of the research area had moderate to low LD, with only 6% having very high to high LD, which has important GWP. The LD

is most distinct in the Kohat and Waziristan-Sulaiman ranges in the north and the Marwat, Bittani, and Shinghar ranges in the south, west, and east, respectively.

### Slope

The slope is a vital factor in evaluating GWP, as it affects water penetration, surface water flow, groundwater recharge, and aquifer storage. Steeper slopes commonly lead to low penetration, storage, and recharge, whereas gentle slopes support good penetration and high GPW (Magesh et al., 2012; Selvam et al., 2015; Mumtaz et al., 2019). High slopes often have rapid runoff, limiting water retention and recharge, whereas low slopes encourage deeper water penetration and retention. Table 5 and Fig. 5 show the numerous slope classes and their particular attention areas. The findings show that very high-class 0-0.8° slope covers 4134.61 km<sup>2</sup> (95.0881% of the total area), high 8.1-16°

**Fig. 5.** Map showing the slope in degrees

**Table 5.** Slope classes in degrees and area in km<sup>2</sup>

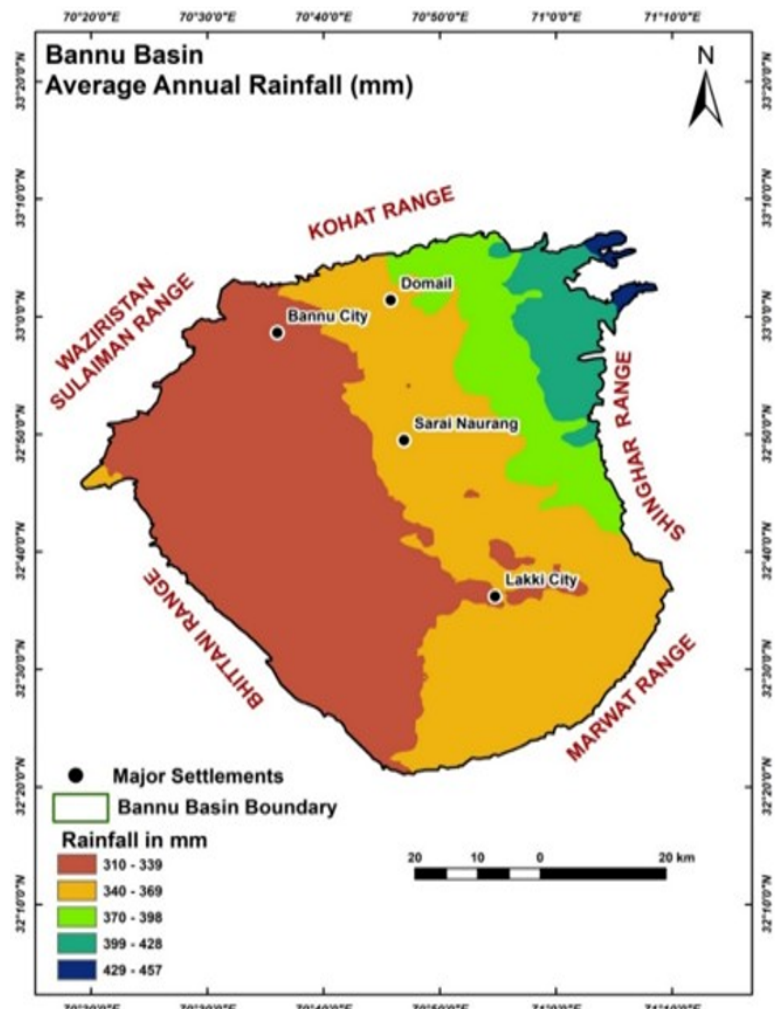
Slope classes	Slope in degree	Area in km <sup>2</sup>	%
Flat	0-0.8°	4134.61	95.0881
Gentle slope	8.1 - 16°	205.19	4.7190
Moderate slope	17 - 24°	7.816	0.1798
Steep slope	25 - 35°	0.555	0.0128
Very Steep slope	35<	0.019	0.0004
Total		4360.19	100

slope covers 205.19 km<sup>2</sup> (4.7190%), moderate 17-24° slope covers 7.816 km<sup>2</sup> (0.1798) low 25-32° slope covers 0.555 km<sup>2</sup> (0.0128%), and very low >32° slope covers 0.019 km<sup>2</sup> (0.0004%). Fig. 5 shows the spatial distribution of the slope classes. These classes were assigned weighted scores depending on their influence on the GWP. Flat and gentle slopes were assigned a value of 2 based on their essential role in water

recharge and preservation, whereas moderate slopes were assigned a weight of 1, indicating their slight impact on GWP (Mandal et al., 2021; Nasir et al., 2021). The results demonstrate that the majority of the study area is characterized by gentle to flat slopes, providing a robust potential for groundwater recharge. Table 5 emphasizes that a large area is favorable for groundwater development, based on the slope's characteristics.

### Rainfall

According to Minh et al. (2019), rainfall is the primary source of groundwater recharge, assists in the penetration of water into the soil, and refills underground water aquifers. The quantity and concentration of rainfall are essential for detecting groundwater regions. In regions with substantial rainfall, groundwater recharge potential is high, whereas areas with scant rainfall have poor recharge potential. For this

**Fig. 6.** Rainfall map showing rainfall class intervals in millimeters

**Table 6.** Qualitative ranking of rainfall and area km<sup>2</sup>

Rainfall (mm)	Qualitative Ranking	Area in km <sup>2</sup>	%
310 - 339	Very low	1948.94	45
340 - 369	Low	1652.88	38
370 - 398	Moderate	456.6	10
399 - 428	High	273.07	6
429 - 457	Very High	28.8	1
Total		4360	100

research, rainfall data for the district of Bannu were acquired from the meteorological station in Peshawar and the WorldClim website. The data were categorized into rainfall classes using equal-interval techniques in ArcGIS. Fig. 6 and Table 6 show the area and percentage of the research area enclosed by each rainfall class, respectively. The Bannu Basin experiences very low rainfall, ranging from 310 to 457 mm, which is inadequate for significant groundwater recharge. Rainfall was categorized as follows: very low (310-339 mm), accounting for 1948.94 km<sup>2</sup> (45%), Low (340-369 mm), accounting for 1652.88 km<sup>2</sup> (38%), Moderate (370-398 mm) 456.6 km<sup>2</sup> (10%), high (399-428 mm) 273 km<sup>2</sup> (6%), and very high (429-457 mm) 28.8 km<sup>2</sup> (1%) of the total areas. To assess GWP recharge, each rainfall class was assigned a weighted value depending on its influence. Higher scores were assigned to high-rainfall zones, whereas lower scores were assigned to low-rainfall areas in previous studies (Nasir et al., 2021). Fig. 6 illustrates the spatial classification of rainfall and provides details on the various rainfall classes.

### Land use/Land cover (LULC)

LULC significantly affects groundwater recharge potential. According to Yin et al. (2011), land use refers to anthropogenic activities on land, whereas land cover relates to the natural surface cover. For this study, Landsat OLI satellite imagery for the Bannu Basin, with a 30m resolution, was acquired from the USGS website. Supervised classification maximum likelihood was employed using ArcGIS to categorize the area into six LULC classes. Barren land accounted for 43.12 km<sup>2</sup> (0.98%), built-up areas 299.74 km<sup>2</sup> (6.87%), cultivated land 908 km<sup>2</sup> (20.82%), rangeland 3092.18 km<sup>2</sup> (70.91%), vegetation 3.82 km<sup>2</sup> (0.087), and water 13.4 km<sup>2</sup> (0.30%). Rangeland is the main land cover, accounting for 71% of the total area (Table 7). This land is naturally covered by vegetation such as *Acacia arabica*, *A. nilotica*, *A. modesta*, jujube, and shrubs. LULC plays an essential role in altering natural phenomena, such as water flow and infiltration, thereby affecting groundwater recharge potential. Various LULC classes were inversely correlated with groundwater recharge. Based on expert opinion and literature, each category was assigned a weight reflecting its influence on GWP: Vegetation, cultivated land, and water were assigned a weight of 2 owing to their high impact on GWP, Barren land and rangeland were assigned a weight of 1 due to their low impact; and built-up areas were assigned a weight of 0 due to their lack of effect on GWP. Fig. 7 shows the spatial distribution of different LULC classes in the Bannu Basin.

**Table 7.** LULC classes in km<sup>2</sup> and qualitative ranking

LULC classes	Qualitative Ranking	Area in km <sup>2</sup>	%
Built up Area	Very Low	299.7441	6.87
Rangeland	Moderate	3092.1894	70.91
Barren Land	Low	43.1415	0.98
Cultivated Land	High	908.0109	20.82
Water	Very High	13.4037	0.30
Vegetation	High	3.8205	0.087
Total		4360.3101	100

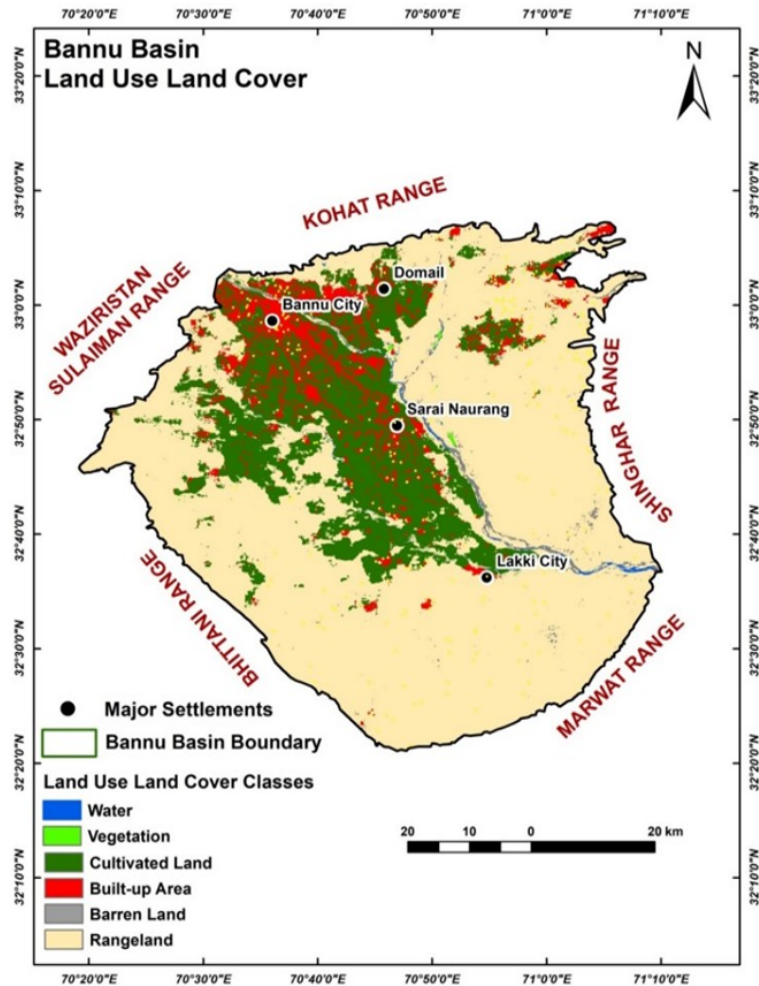


Fig. 7. Spatial distribution of various LULC classes

### Elevation

Elevation is a leading factor in GWP because of its effects on water movement, the hydrological cycle, and precipitation. High elevations receive additional precipitation, which improves groundwater recharge. Low elevations receive low precipitation. In addition, the form of precipitation, including snow and rain, and periodic rainfall can greatly influence recharge. High elevations also show different soil categories, which may differ in water infiltration, permeability, and retention. Different soil and landscape types border Bannu Basin. The central part of the basin mainly consists of alluvial soils deposited by the Gambilla/Tochi, Kurrum, and Khaisore Rivers. To evaluate the impact of elevation on GWP recharge, we used a 30 m-resolution shuttle radar topographic mission (SRTM) dataset to produce a terrain map. Table 8 and Fig. 8 show the classes and their specific area percentages. The elevation of the research area varied from 211 to 826 m and

was classified into five categories. Such as very high accounts 211-334 m cover 2023.03 km<sup>2</sup> with 47.57% of the total area, high ranging from 335-45 m cover 1875.26 km<sup>2</sup> with 43.47%), moderate (458-580): 335.30 km<sup>2</sup> (8.24%), low ranging from 581-703 m cover 26.22 km<sup>2</sup> with 0.65%), very low (704-826 m) cover area 3.39

Table. 8. Elevation classes and qualitative ranking potential

Elevation Classes (m)	Qualitative Elevation Ranking for GW potentiality	Area in km <sup>2</sup>	Percentage of total area
211-334	Very High	2023.028	47.57
335-457	High	1875.265	43.47
458-580	Moderate	335.3066	8.24
581-703	Low	26.2248	0.65
704-826	Very low	3.395504	0.08
Total		4360.20	100

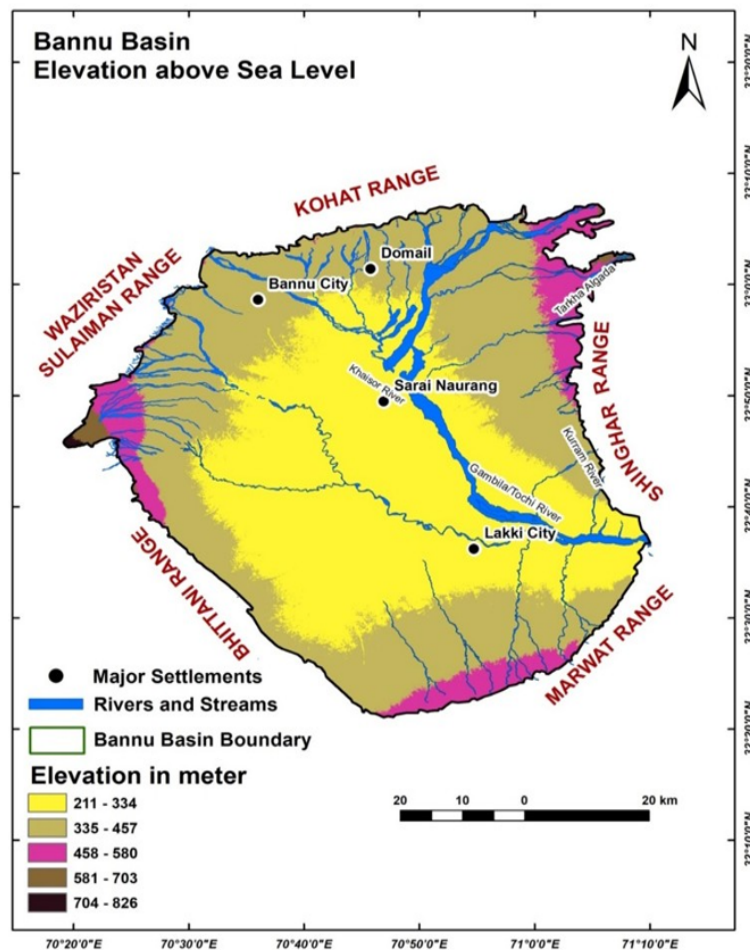


Fig. 8. Spatial distributions of various elevation classes

km<sup>2</sup> (0.08%). A weight was assigned to each class based on its influence on GWP recharge. In the groundwater study, higher values and weights were assigned to low-elevation areas, as they are more suitable for groundwater storage and recharge due to lower gravity and water streams, which cover 91.04% of the total area. Moderate was assigned 1 due to a minor impact on GWP, covering 8.24% of the area. Very low and low were assigned a value of 0,

as they had a slight to no influence on GWP, covering 0.73% of the total area.

### Geology

Geology plays a vital role in groundwater (GW) recharge, particularly affecting the penetration and movement of water within groundwater aquifers. According to [Ramu et al. \(2015\)](#), the geology of a region is crucial for detecting potential groundwater recharge. The hydraulic

Table 9. Geology classes and qualitative ranking for GWP and area in km<sup>2</sup>

Geology Classes	Qualitative Elevation Ranking for GPW	Area in km <sup>2</sup>	Percentage
Alluvium, Sandstone,	Very High	3699.1	84.84
Water	Very High	7.17	0.16
Conglomerate, Mudstone	High	488.2	11.20
Calcareous Shale, Limestone	Moderate	67.01	1.54
Red Clastic Sandstone, Shale	Moderate	83.7	1.92
Dolomite, Quartzite	low	15.02	0.34
Total		4360.20	100

slope, which controls the flow of water from the recharge to the release zones, is directly affected by the penetration of geological development (Manikandan and Moganraj, 2014). For this study, a geological map of northern Pakistan was used to evaluate the geology of the Bannu Basin. The geology was categorized and digitized into various geological formations, depending on their potential to contribute to groundwater recharge. The main geological structures in the research area consist of mudstone, alluvium, sandstone, conglomerate, shale, siltstone, quartzite, dolomite, and limestone. The Bannu Basin geology was classified into six categories, with their consistent areas and percentages described in Table 9 and Fig. 9.

Alluvium and sandstone cover 3699.10 km<sup>2</sup>, which is 84.84% of the total area, calcareous shale and limestone cover 67.01 km<sup>2</sup> (1.54%), conglomerate and mudstone cover 488.20 km<sup>2</sup>, which is 11.20%, clastic sandstone red, and shale span covering 83.72 km<sup>2</sup> (1.92%), dolomite and quartzite cover 12.08 km<sup>2</sup> (0.28%), and water

covers 7.17 km<sup>2</sup> (0.16%). The main part of the study is enclosed by alluvium and sandstone, which are more porous and favorable for groundwater recharge, particularly as rivers drain them from the adjacent mountain ranges. Each geological class was assigned a weight based on its influence on groundwater recharge. Water, sandstone, alluvium, conglomerate, and mudstone were assigned a score of 2 owing to their high potential and penetration for important groundwater recharge. Red clastic sandstone, shale, limestone, and calcareous were assigned a weight value of 1, reflecting their low influence on GW recharge. Fig. 9 shows the spatial distribution of the numerous geological formations in the Bannu Basin, providing a sense of the area's varying groundwater recharge potential.

### Soil

Soil texture is an important factor affecting water provision, penetration, and GWP recharge. Soil texture refers to the proportions of silt, clay, and

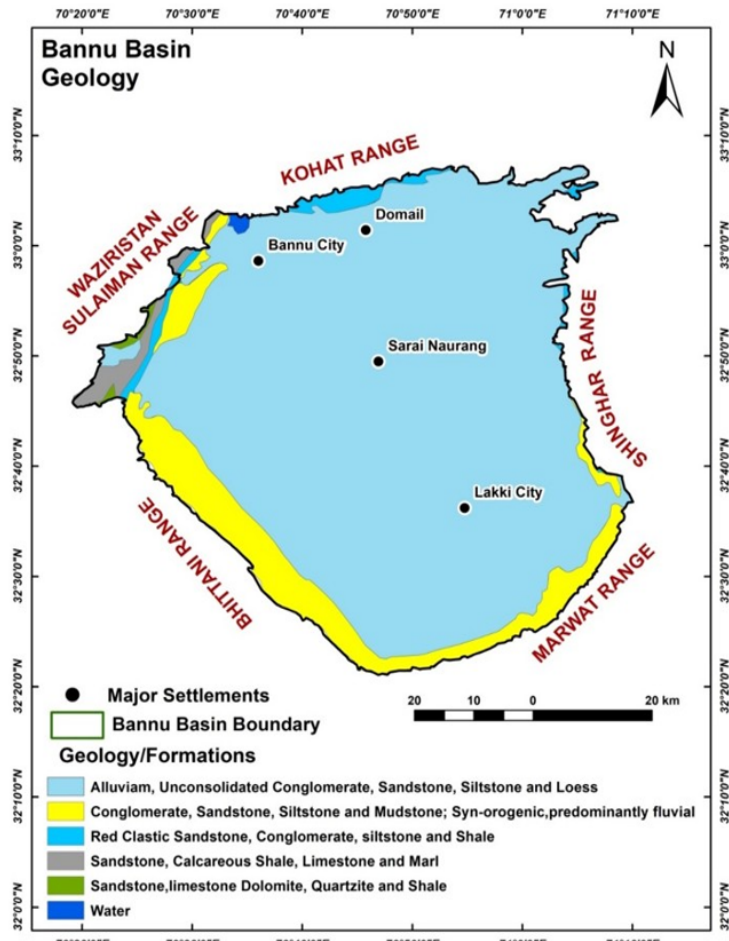


Fig. 9. Geology Map showing different classes

sand in the soil, which directly affect infiltration capacity, porosity, permeability, and water retention capacity. Soil with uneven textures, such as sandy soil, allows water to penetrate rapidly and is favorable for groundwater recharge, whereas fine soil textures, such as clay, have low penetration and resist water flow, consequently limiting recharge (Ahmad et al., 2020; Ma et al., 2016). Soil penetration, which affects the soil's ability to diffuse water, plays a major role in determining the extent of groundwater recharge. Sandy soils, with their large particles, permit rapid drainage and ease recharge, whereas clay soils, with their small particles, slow drainage and reduce recharge potential. Hence, soil characteristics are vital for assessing GWP recharges. The soil data for

this research were acquired from the Food and Agriculture Organization (FAO), version 3.6, which was completed in January 2003. The study area consisted of two main soil types: haplic xerosols and lithosols. Lithosols consist of rock fragments, gravel, and stones that mainly originate in areas where bedrock is near the surface. They have poor soil development due to unweathered rock, resulting in weak soil retention and limited penetration. Haplic Xerosols are found in semiarid and arid climates and are characterized by limited leaching, poor soil horizon development, and variable salt accumulation. Xerosols commonly grow in area with high evaporation and low precipitation, affecting their water preservation and dimensions. Table 10 and Fig. 10 illustrate

Table. 10. Soil composition

Soil Type	Abbreviations	sand % topsoil	silt % topsoil	clay % topsoil	OC % topsoil
Haplic Xerosols	XH	54.8	20.6	24.9	0.53
Lithosols	I	58.9	16.2	24.9	0.97

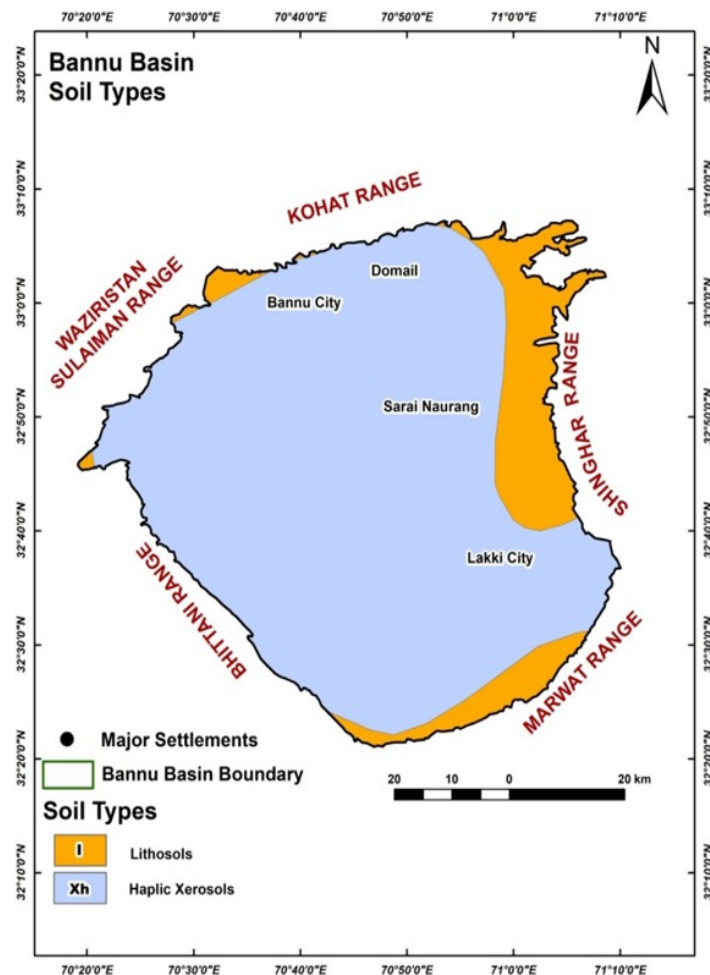


Fig. 10. Soil texture map

the distribution of soil types and their areas in the study area. Haplic xerosols covered 3751 km<sup>2</sup>, or 86.03% of the total area. Lithosols accounted for 609.14 km<sup>2</sup> or 13.97% of the total area. A weighted value of 2 was assigned to haplic xerosols because of their important influence on groundwater recharge, whereas lithosols were assigned a low weight because of their low capability to accumulate and collect water. This categorization assists in determining the significance of soil characteristics in assessing the GWP recharge of the area (Manikandan and Moganraj, 2024; Mandal et al., 2021).

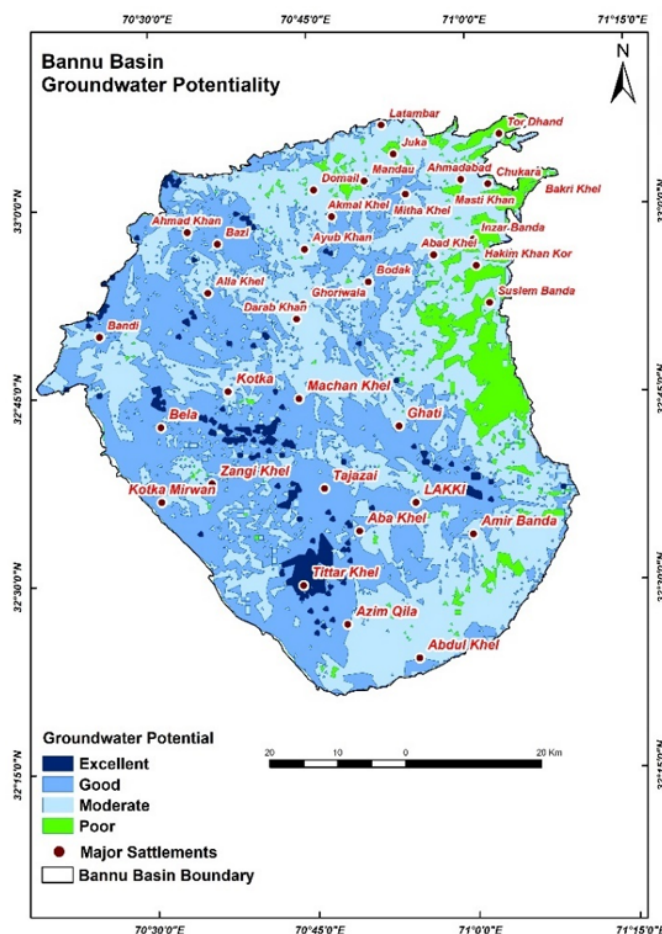
### GWP Map

Table 11 and Fig. 11 show the areas and percentages of various GWP zones within the Bannu Basin. The spatial distribution of the GWP zones is shown in Fig.11. Table 11 and Fig. 11 show that the majority of the Bannu Basin has a good GWP, covering 2089.41 km<sup>2</sup>, which accounts for 47.92% of its total area. Excellent GWP was 190.643 km<sup>2</sup>, accounting for 4.56% of the total area, whereas moderate

GWP covers 1689.219 km<sup>2</sup> and occupies 38.96% of the area. Poor GWP covers 350.633 km<sup>2</sup>, or 8.57% of the entire basin. Fig. 11 shows that the spatial distribution of GWP is highly adjustable and uneven. The major portion of the excellent GWP is focused in the central part of the basin, incredibly close to perennial streams and major rivers. A significant portion of the GWP was detected in the southwestern region of the basin. A comparative study of the GWP map with an elevation range of 211-234 m above sea level, slopes varying from 0°-8°, very high stream densities, and moderate to

**Table. 11.** GWP classes area in km<sup>2</sup>

GWP Classes	Area ins km <sup>2</sup>	%
Excellent	198.64	4.56
Good	2089.41	47.92
Moderate	1698.52	38.96
Poor	373.63	8.57
Total	4360.20	100



**Fig. 11.** A GWP zone map is shown

high lineament. However, rainfall and soil did not seem to play a key role in the basin's GWP because of the area's invariability.

The amount of rainfall in the study area was recorded 310-356.97 mm, and the soil types in the Bannu Basin are haplic xerosols, which account for 86.3% of the Bannu Basin with high GWP. A good GWP was located in the central part of the basin, which is typically enclosed by water bodies. The majority of the moderate zone was situated in the northeastern and southern portions of the study area. The area with poor GWP was mainly situated in the eastern part of the study area, spreading along a significant portion of the eastern Bannu Basin. This area has a high-to-moderate elevation range of 458-580 m above sea level and is considered to have low to very low stream and lineman densities. Overall, the analysis revealed an accurate distribution of GWP across the study area, with 52% of the area falling into the good-to-excellent GWP categories.

### Validation of GWP Results

A field survey was conducted to gather GWT data from all accessible tube wells and various dug wells in the area to confirm the study results. A Magellan Triton 1500 GPS unit was used for data collection, and the coordinates of both the tube and the dug wells were recorded, along with the corresponding GWT depths. To determine the depth of the GWT, field operators took instantaneous measurements from tube wells and local wells. The XY coordinates were collected in the field, saved as a GPS file, imported into ArcMap 10.8, and saved as a point layer. Point data were presented on the GWP layer and compared for validation. Table 11 and Fig. 11 illustrate the areas under various GWT zones, whereas the spatial distribution of GW depth is shown in Fig. 12.

Table 12 and Fig.12 show that the GWT depth varies from a very shallow range of 25-411+ feet. To achieve this, the GWT depth data were categorized into four classes. The area where the

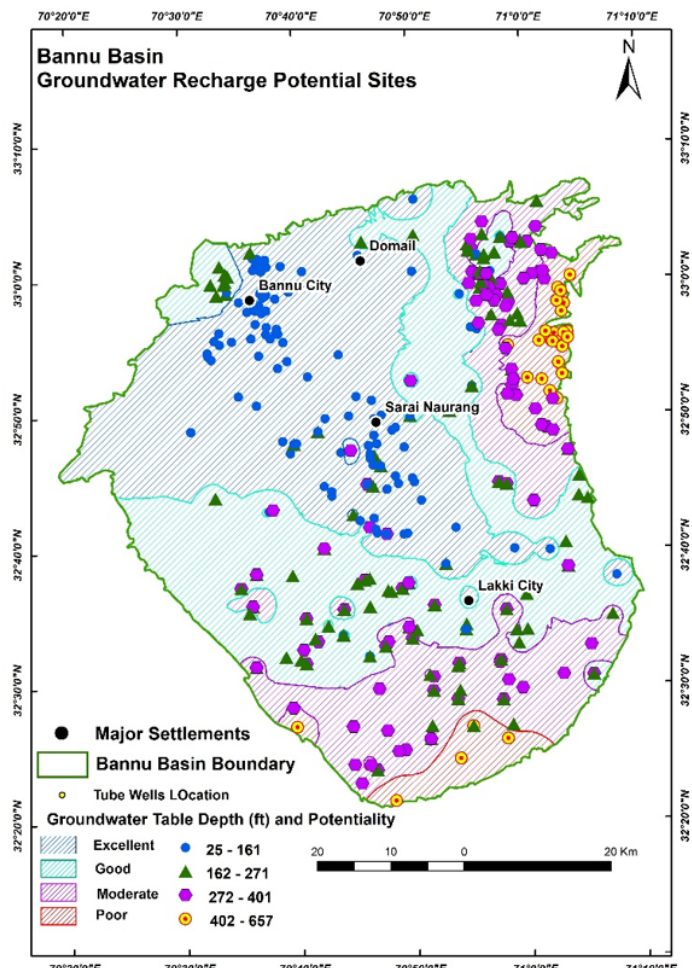


Fig. 12. Spatial distribution of surveyed tube wells and GWT depths

GWT depth ranges from 25-261 feet accounts for 1594.72 km<sup>2</sup> (36.57%), and the GWT depth range from 162-271 feet accounts for 1465.16 km<sup>2</sup> (33.60%) of the total area. However, the zone of GWT depth range from 272-401 feet accounts for 963.5 km<sup>2</sup> (22.10%), and the GWT depth range of 402-657 feet accounts for 336.82 km<sup>2</sup> (7.72%) of the total area. The outputs showed that the majority of the surface GWT was located in the basin's central region, whereas the deep GWT originated in the basin's border areas. The GWT zones are similar to the GWP zones. Consequently, the analysis of both GWP and GWT zones illustrated that most wells with surface GWT depths are located within areas of excellent to good GWP, whereas deep wells are situated in zones with poor GWP.

*Delineation of Groundwater Recharge Sites*

Groundwater (GW) recharge site recognition and delineation involve mapping areas where

**Table. 12.** GWT depth and associated areas within the Bannu Basin

GWT depth in feet	Tube wells No	Area in km <sup>2</sup>	%
25-161	167	1594.72	36.57
162-271	158	1465.16	33.60
272-401	124	963.5	22.10
402-657	41	336.82	7.72
	490	4360.2	100.00

water can penetrate the ground and replenish groundwater basins. This procedure is crucial for the effective and sustainable management of water resources, particularly in regions where groundwater is the key source of irrigation and drinking water. This study aimed to identify potential groundwater recharge locations within the Bannu Basin. Eight parameters were examined using the MIF method to achieve this. These parameters include soil, LULC, DD and LD, rainfall, topography, geology, and runoff potential. Although these parameters were broadly assessed for GWP, diverse ranking approaches were applied for LULC and DD, with runoff potential being the main parameter in the study. A high DD characteristically indicates a lower penetrable surface, leading

to increased surface runoff and reduced groundwater recharge potential (GWRP). The DD in the study area ranged from 0.081 to 0.55 km/km<sup>2</sup>. It was categorized into five classes based on its impact on GWP recharge: very low (0.55-0.9), high (0.38-0.55), moderate (0.23-0.37), low (0.082-0.22), and very low (0-0.081) applicability of groundwater recharge (Hussaini et al., 2022). The computed potential runoff for the Bannu Basin ranged from 305.41 to 349 mm, with greater runoff potential representing lower suitability for groundwater recharge. Areas with higher runoff potential are ideal for RWH and groundwater recharge. The runoff potential was classified into five classes: very low (305.41 mm), low (308.71 mm), moderate (319 .70 mm), high (329.06 mm), and very high (349.54 mm) potential for GW recharge. Locations with high and very high runoff potentials were given a weighted value of 2, whereas those with moderate and low potentials were given a score of 1. Tables 13 and 14 show the comparative weight score values, the projected weights assigned to each IP, the quantity ranking of each subclass, and the weight percentage for the weighted overlay analysis.

#### **Map of Groundwater Recharge Sites**

The results of groundwater recharge locations are presented in Table 15, which classifies the area into five categories based on recharge potential: very poor, poor, moderate, good, and excellent (Nasir et al., 2018; Zghibi et al., 2020; Mandal et al., 2021). The details in Table 15 and Fig.13 indicate that most parts of the research area showed good to moderate GWP. Notably, areas with moderate and good GWP cover 3949.92 km<sup>2</sup>, accounting for 90.59% of the total area. A minor portion of 50.14 km<sup>2</sup> is categorized as excellent GWP, accounting for 1.15%. In contrast, areas with poor and very poor GWP cover 340.3 km<sup>2</sup> and 19.82 km<sup>2</sup>, accounting for 7.81% and 0.45% of the total area, respectively. Fig. 13 shows the spatial distribution of GWP recharge across the Bannu Basin. The results show that the distribution of GWP recharge follows a pattern similar to that of GW recharge. Excellent GWP recharge was focused in a minor area in the southwestern portion of the basin, whereas poor recharge potential originated in

**Table. 13.** Weight scores were assigned to various subclasses of all the variable parameters

A	B	C	D	E	F	G
IP	Sub categories of the IP	Qualitative Ranking	Major effect (A)	Minor Effect (B)	relative sum of Effects (A+B)	Proposed weightage of each IP (A+B)/ $\Sigma(A+B) \times 100$
DD m/Km <sup>2</sup>	0.55 – 0.9	Very High	-	-	6	12
	0.38 – 0.55	High	-	1		
	0.23 – 0.37	Moderate	-	1		
	0.082 - 0.22	Low	2	-		
	0 - 0.081	Very Low	2	-		
LD km/Km <sup>2</sup>	0.62 – 0.77	Very High	2	-	6	12
	0.47 – 0.61	High	2	-		
	0.32 – 0.46	Moderate	-	1		
	0.16 – 0.31	Low	-	1		
	0 – 0.15	Very Low	-	-		
LULC	Water	Very High	2	-	8	16
	Rangeland	High	2	-		
	Barren land	High	2	-		
	Cultivated land	Moderate	1	-		
	Vegetation	Low	1	-		
	Built-up Area	Very Low	-	-		
Geology	Water	Very High	2	-	8	16
	Alluvium, Sandstone	Very High	2	-		
	Conglomerate, Mudstone	High	2	-		
	Calcareous shale, Limestone	Moderate	-	1		
	Red-Clastic Sandstone, Shale	Moderate	-	1		
	Dolomite, Quartzite	Low	-	-		
Soil	Lithosols	Very High	2	-	4	8
	Haplic Xerosols	High	2	-		
Rainfall in mm.	429 – 457	Very High	2	-	6	12
	399 – 428	High	2	-		
	370 – 398	Moderate	-	1		
	340 – 369	Low	-	1		
	310- 339	Very Low	-	-		
Topography (Slope) In Degrees.	0 – 8	Very High	2	-	6	12
	9 – 16	High	2	-		
	17 – 24	Moderate	-	1		
	24 – 32	Low	-	1		
	32 – 35.2	Very Low	-	-		
Recharge Potential	305.41	Very Low	-	-	6	12
	308.71	Low	-	1		
	319.70	Moderate	-	1		
	329.06	High	2	-		
	349.54	Very High	2	-		
			$\Sigma A=38$	$\Sigma B=12$	$\Sigma A+B=50$	$\Sigma 100$

**Table 14.** Thematic layers and corresponding scores

IP	Sub categories of the IP	Qualitative Ranking	Proposed weightage of IP	Quantitative Ranking	Influence % for weighted overlay analysis
DD m/km <sup>2</sup>	0.55 – 0.9	Very High	12	12	10
	0.38 – 0.55	High		9	
	0.23 – 0.37	Moderate		6	
	0.082 - 0.22	Low		3	
	0 - 0.081	Very Low		1	
LD km/km <sup>2</sup>	0.62 – 0.77	Very High	12	12	10
	0.47 – 0.61	High		9	
	0.32 – 0.46	Moderate		6	
	0.16 – 0.31	Low		3	
	0 – 0.15	Very Low		1	
LULC	Water	Very High	16	16	10
	Rangeland	High		14	
	Barren land	High		11	
	Cultivated land	Moderate		7	
	Vegetation	Low		3	
	Built-up Area	Very Low		1	
Geology	Water	Very High	16	16	10
	Alluvium, Sandstone	Very High		16	
	Conglomerate, Mudstone	High		14	
	Calcareous shale, Limestone	Moderate		11	
	Red-Clastic Sandstone, Shale	Moderate		7	
	Dolomite, Quartzite	Low		3	
	Lithosols	Very High		8	15
Soil	Haplic Xerosols	High		4	
Rainfall in mm.	429 – 457	Very High	12	12	15
	399 – 428	High		9	
	370 – 398	Moderate		6	
	340 – 369	Low		3	
	310- 339	Very Low		1	
Topography (Slope) In Degrees.	0 – 8	Very High	12	12	10
	9 – 16	High		9	
	17 – 24	Moderate		6	
	24 – 32	Low		3	
	32 – 35.2	Very Low		1	
Recharge Potential	305.41	Very Low	12	12	20
	308.71	Low		9	
	319.70	Moderate		6	
	329.06	High		3	
	349.54	Very High		1	
			$\Sigma 100$		$\Sigma 100$

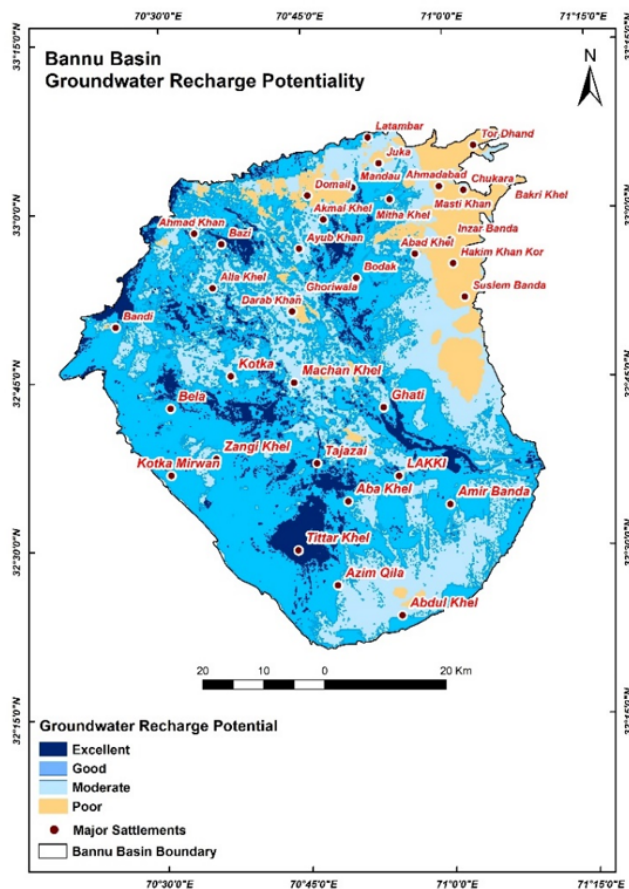


**Fig. 13.** Spatial distributions of groundwater recharge potential zones in the Bannu Basin

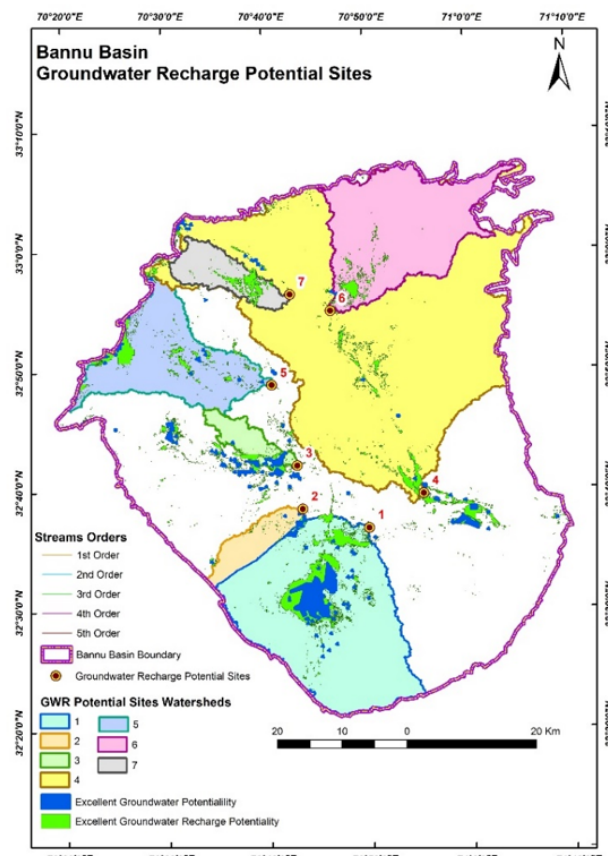


**Fig. 14.** Potential sites identified for groundwater aquifer recharge structures

**Table 15.** Groundwater recharge zone area in km<sup>2</sup>

Classes	Area in km <sup>2</sup>	%
Excellent	50.14	1.15
Good	1828.75	41.94
Moderate	2121.17	48.65
Poor	340.33	7.81
Total	4360.20	100.00

areas characterized by low permeability and limited infiltration capacity, covering 340.33 km<sup>2</sup> and 19.82 km<sup>2</sup>, or 7.81% and 0.45% of the total area, respectively. Fig. 14 illustrates the potential sites for groundwater aquifer recharge.

## CONCLUSIONS

Evaluating GWP and recharge is essential for effective water resource management. By systematically considering the geological, hydrological, and climatic factors that influence groundwater accessibility, decision-makers can formulate well-informed policies to safeguard the long-term viability of aquifers. Classifying areas with high GWP enables targeted and effective management of these valuable resources. Thus, it is necessary to support numerous anthropogenic activities, such as domestic, agricultural, and industrial uses. However, a careful approach to groundwater extraction can prevent overexploitation and its adverse impacts on the sustainability of groundwater aquifers. Groundwater recharge analysis is essential because it provides insights into the replenishment of aquifers. By evaluating factors influencing recharge - such as land-use changes, precipitation, soil permeability, and runoff potential - planners can implement measures to increase recharge rates. This may include land management practices, watershed management initiatives, and artificial recharge approaches that help maintain a strong balance between groundwater extraction and recharge. GWP and delineation zones in the Bannu Basin were determined using GIS, RS, MIF, and weighted overlay analysis approaches, which proved efficient in terms of time, labor, and cost savings and therefore enabled rapid decision-making for the viable management of water resources. Satellite images, geological and

topographical maps, and traditional data were used to produce thematic layers such as LULC, soil, DD, LD, topography, rainfall, geology, and runoff potential. The different thematic layers were assigned appropriate weight scores using the MIF approach within a unified GIS environment to produce the GWP zone map for the study area. According to the GWP map, the Bannu Basin was classified into four classes: 'good,' excellent, 'moderate,' and 'poor.' Thus, significant GWP accounted for 47.92% (of the total area), excellent GWP for 4.56%, moderate GWP for 38.96%, and poor GWP for over 8.57% of the total area. The results revealed that 90.59% of the Bannu Basin has moderate-to-significant groundwater recharge potential. The findings of this study can serve as a basis for policy formulation and the implementation of various human activities, such as domestic use, industry, and agriculture. However, understanding the hydrological, geological, and climatic factors that govern groundwater supply can help decision-makers develop proactive plans to safeguard the long-term sustainability of groundwater aquifers.

Systematic study and resilient management planning are essential to address changing environmental conditions and ensure the sustainability of groundwater resources for future generations. Nevertheless, technological, scientific, and public engagement developments can promote the sustainable and responsible management of groundwater resources, ensuring continued access to this vital resource for global water provision. This empirical approach for examining groundwater zones uses RS and GIS to identify potential groundwater zones. These techniques can be broadly applied across large areas with uneven topography to analyze suitable site selection for GWP and recharge.

## ACKNOWLEDGEMENT

The authors acknowledge the Department of Geography, University of Peshawar; the Department of Geography, Islamia College Peshawar, Pakistan; and Tishk International University, Erbil, Iraq.

## Authors Contribution

Muhammad Jamal Nasir; Supervision, original

draft writing, analysis, Jawad Ur Rahman; Methodology, Investigation, writing, Abdur Raziq; rewriting, correction of English, reviewing the manuscript. Ayad M. Fadhil Al-Quraishi; editing, extensive reviewing, and finalizing the manuscript.

### Funding:

All authors declared that no grants or funds were received during the preparation of this paper.

### Data Availability

The data will be available on request.

### Declarations

**Ethical Approval** All authors acknowledge that this paper has not been published and is not under consideration, and that no plagiarism has occurred.

**Consent to Participate** All authors agreed to participate in this study.

**Consent to Publish** All authors agree to publish this manuscript in this journal.

**Competing Interests:** The authors declare no conflicts of interest.

## REFERENCE

Abdullah, M., Khan, S., Ali, R. 2022. Assessment of water conservation techniques in semi-arid regions. *Water Resources Journal*, Vol. 17(3), p. 134-145.

Adham, M.I., Shirazi, S.M., Othman, F., Rahman, S., Yusop, Z., Ismail, Z. 2014. Runoff Potentiality of a Watershed through SCS and Functional Data Analysis Technique. *The Scientific World Journal*, vol. 2014(1), 379763. <https://doi.org/10.1155/2014/379763>

Adimalla, N., Li, P., Venkatayogi, S. 2018. Hydrogeochemical Evaluation of Groundwater Quality for Drinking and Irrigation Purposes and Integrated Interpretation with Water Quality Index Studies. *Environmental Processes*, v. 5(2), p. 363-383. <https://doi.org/10.1007/s40710-018-0297-4>

Afzal, M., Liu, T., Butt, A.Q., Nadeem, A.A., Ali, S., Pan, X. 2023. Geospatial Assessment of Managed Aquifer Recharge Potential Sites in Punjab, Pakistan. *Remote Sensing*, v. 15(16), p. 3988. <https://doi.org/10.3390/rs15163988>

Ahmad, I., Dar, M.A., Andualem, T.G., Teka, A.H., Tolosa, A.T. 2020. GIS-based Multi-Criteria Evaluation for Deciphering of Groundwater Potential. *Journal of the Indian Society of Remote Sensing*, vol. 48(2), p. 305-313. <https://doi.org/10.1007/s12524-019-01078-3>

Ahmad, R., Gabriel, H.F., Alam, F., Zarin, R., Raziq, A., Nouman, M., Liou, Y.A. 2024. Remote Sensing and GIS Based Multi-Criteria Analysis Approach with Application of AHP and FAHP for Structures Suitability of Rainwater Harvesting Structures in Lai Nullah, Rawalpindi, Pakistan. *Urban Climate*, vol. 53, 101817. <https://doi.org/10.1016/j.uclim.2024.101817>

Akudo, E.O., Ifediegwu, S.I., Ahmed, J.B., Aigbadon, G.O. 2024. Identifying Groundwater Potential Regions in Sokoto Basin, Northwestern Nigeria: An Integrated Remote Sensing, GIS, and MIF Techniques. *Journal of the Indian Society of Remote Sensing*, vol. 52, p. 1201-1222. <https://doi.org/10.1007/s12524-024-01872-8>

Akudo, E.O., Ozulu, G.U., Osogbue, L.E. 2010. Quality Assessments of Groundwater from Selected Refuse Dumpsites Areas in Warri. *Environmental Research Journal*, v. 4(4), p. 281-285. <https://doi.org/10.3923/erj.2010.281.285>

Alam, F., Azmat, M., Zarin, R., Ahmad, S., Raziq, A., Young, H.W.V., Nguyen, K.A., Liou, Y.A. 2022. Identification of Potential Natural Aquifer Recharge Sites in Islamabad, Pakistan, by Integrating GIS and RS Techniques. *Remote Sensing*, v. 14(23), p. 6051. <https://doi.org/10.3390/rs14236051>

Dar, I.A., Sankar, K., Dar, M.A. 2010. Deciphering Groundwater Potential Zones in Hard Rock Terrain Using Geospatial Technology. *Environmental Monitoring and Assessment*, v. 173, p. 597-610. <https://doi.org/10.1007/s10661-010-1407-6>

Datta, A., Gaikwad, H., Kadam, A., Umrikar, B.N. 2020. Evaluation of Groundwater Prolific Zones in the Unconfined Basaltic

Aquifers of Western India Using Geospatial Modeling and MIF Technique. *Modeling Earth Systems and Environment*, vol. 6, p. 1807-1821.  
<https://doi.org/10.1007/s40808-020-00791-0>

Deshmukh, K.K. 2011. Assessment of Groundwater Quality in Sangamner Area for Sustainable Agricultural Water Use Planning. *International Journal of Chemical Sciences*, v. 9(3), p. 1486-1500.

Ebrahimian, M. 2012. Application of NRCS-Curve Number Method for Runoff Estimation in a Mountainous Watershed. *Caspian Journal of Environmental Sciences*, v. 10(1), p. 103-114.

Etikala, B., Golla, V., Li, P., Renati, S. 2019. Deciphering Groundwater Potential Zones Using MIF Technique and GIS: A Study from Tirupati Area, Chittoor District, Andhra Pradesh, India. *HydroResearch*, vol. 1, p. 1-7. <https://doi.org/10.1016/j.hydres.2019.04.001>

Fagbohun, B.J. 2018. Integrating GIS and Multi-Influencing Factor Technique for Delineation of Potential Groundwater Recharge Zones in Parts of Ilesha Schist Belt, Southwestern Nigeria. *Environmental Earth Sciences*, v. 77(3), 69. <https://doi.org/10.1007/s12665-018-7229-5>

Faheem, H., Khattak, Z., Islam, F., Ali, R., Khan, R., Khan, I., Eldin, E.T. 2023. Groundwater potential zone mapping using geographic information systems and multi-influencing factors: A case study of the Kohat District, Khyber Pakhtunkhwa. *Frontiers in Earth Science*, vol. 11, 1097484. <https://doi.org/10.3389/feart.2023.1097484>

Gaikwad, H., Shaikh, H., Umrikar, B. 2018. Evaluation of Groundwater Quality for Domestic and Irrigation Suitability from Upper Bhima Basin Western India: A Hydrogeochemical Perspective. *Hydrospatial Analysis*, 2018(2), p. 113-123. <https://doi.org/10.21523/gcj3.18020204>

Gumma, M.K., Pavelic, P. 2013. Mapping of Groundwater Potential Zones across Ghana Using Remote Sensing, Geographic Information Systems, and Spatial Modeling. *Environmental Monitoring and Assessment*, vol. 185(4), p. 3561-3579. <https://doi.org/10.1007/s10661-012-2810-y>

Hassan, M., Ali, K.W., Amin, F.R., Ahmad, I., Khan, M.I., Abbas, M. 2016. Economical Perspective of Sustainability in Agriculture and Environment to Achieve Pakistan Vision 2025. *International Journal of Agriculture and Environmental Research*, v. 2(2), p. 113-124.

Hussaini, M.S., Farahmand, A., Shrestha, S., Neupane, S., Abrunhosa, M. 2022. Site Selection for Managed Aquifer Recharge in the City of Kabul, Afghanistan, Using a Multi-Criteria Decision Analysis and Geographic Information System. *Hydrogeology Journal*, vol. 30(1), p. 59-78. <https://doi.org/10.1007/s10040-021-02408-x>

Jalil, A.A., Luyun Jr, R.A., Reyes Jr, A.A.D., Bato, V.A. 2020. Assessment of Groundwater Quality for Irrigation at Malamawi Island, Basilan, Philippines. *Jurnal Penelitian Pengelolaan Daerah Aliran Sungai (Journal of Watershed Management Research)*, v. 4(2), p. 187-200. <https://doi.org/10.20886/jppdas.2020.4.2.187-200>

Jebaraj, S.P., Rajagopal, V. 2024. MIF and AHP Methods for Delineation of Groundwater Potential Zones Using Remote Sensing and GIS Techniques in Tirunelveli, Tenkasi District, India. *Open Geosciences*, v. 16(1), p. 20220619. <https://doi.org/10.1515/geo-2022-0619>

Kalpana, L., Elango, L. 2013. Assessment of Groundwater Quality for Drinking and Irrigation Purposes in Pambar River Sub-Basin, Tamil Nadu. *Environmental Protection*, v. 33(1), p. 1-8.

Khan, D., Raziq, A., Young, H.W.V., Sardar, T., Liou, Y.A. 2022. Identifying Potential Sites for Rainwater Harvesting Structures in Ghazi Tehsil, Khyber Pakhtunkhwa, Pakistan Using Geospatial Approach. *Remote Sensing*, vol. 14(19), p. 5008. <https://doi.org/10.3390/rs14195008>

Khan, U., Faheem, H., Jiang, Z., Wajid, M., Younas, M., Zhang, B. 2021. Integrating a GIS-Based Multi-Influence Factors Model with Hydro-Geophysical Exploration for Groundwater Potential and Hydrogeological Assessment: A Case Study in the Karak Watershed, Northern Pakistan. *Water*, vol. 13(9), 1255.

<https://doi.org/10.3390/w13091255>  
Krishna Kumar, S., Chandrasekar, N., Seralathan, P., Godson, P.S., Magesh, N.S. 2011. Hydrogeochemical Study of Shallow Carbonate Aquifers, Rameswaram Island, India. Environmental Monitoring and Assessment, vol. 184, p. 4127-4138.  
<https://doi.org/10.1007/s10661-011-2249-6>  
Ma, W., Zhang, X., Zhen, Q., Zhang, Y. 2016. Effect of Soil Texture on Water Infiltration in Semiarid Reclaimed Land. Water Quality Research Journal, vol. 51(1), p. 33-41. <https://doi.org/10.2166/wqrjc.2015.025>

Magesh, N.S., Chandrasekar, N., Soundranayagam, J.P. 2012. Delineation of Groundwater Potential Zones in Theni District, Tamil Nadu, Using Remote Sensing, GIS and MIF Techniques. Geoscience Frontiers, vol. 3(2), p. 189-196.  
<https://doi.org/10.1016/j.gsf.2011.10.007>

Mahmoud, S.H., Alazba, A.A. 2016. Integrated Remote Sensing and GIS-Based Approach for Deciphering Groundwater Potential Zones in the Central Region of Saudi Arabia. Environmental Earth Sciences, vol. 75, p. 1-28.  
<https://doi.org/10.1007/s12665-015-5156-2>

Mandal, P., Saha, J., Bhattacharya, S., Paul, S. 2021. Delineation of Groundwater Potential Zones Using the Integration of Geospatial and MIF Techniques: A Case Study on Rarh Region of West Bengal, India. Environmental Challenges, vol. 5, 100396.  
<https://doi.org/10.1016/j.envc.2021.100396>

Manikandan, A.T., Moganraj, M. 2014. Consolidation and Rebound Characteristics of Expansive Soil by Using Lime and Bagasse Ash. International Journal of Research in Engineering and Technology, vol. 3(4), p. 403-411.  
<https://doi.org/10.15623/ijret.2014.0304073>

Minh, H.V.T., Avtar, R., Kumar, P., Tran, D.Q., Ty, T.V., Behera, H.C., Kurasaki, M. 2019. Groundwater Quality Assessment Using Fuzzy-AHP in An Giang Province of Vietnam. Geosciences, vol. 9(8), 330.  
<https://doi.org/10.3390/geosciences9080330>

Mukherjee, P., Singh, C.K., Mukherjee, S. 2012. Delineation of Groundwater Potential Zones in Arid Region of India - A Remote Sensing and GIS Approach. Water Resources Management, v. 26, p. 2643-2672.  
<https://doi.org/10.1007/s11269-012-0038-9>

Multaniya, A.P., Sinha, M.K., Sahu, K.K., Shubham. 2024. Geospatial Technique for the Delineation of Groundwater Potential Zones Using Multi-Criteria-Based AHP and MIF Methods. Water Supply, v. 24(4), p. 1024-1047. <https://doi.org/10.2166/ws.2024.062>

Mumtaz, R., Baig, S., Kazmi, S.S.A., Ahmad, F., Fatima, I., Ghauri, B. 2019. Delineation of Groundwater Prospective Resources by Exploiting Geo-Spatial Decision-Making Techniques for the Kingdom of Saudi Arabia. Neural Computing and Applications, vol. 31, p. 5379-5399.  
<https://doi.org/10.1007/s00521-018-3370-z>

Murugesan, B., Thirunavukkarasu, R., Senapathi, V., Balasubramanian, G. 2012. Application of Remote Sensing and GIS Analysis for Groundwater Potential Zone in Kodaikanal Taluka, South India. Earth Science, v. 7(1), p. 65-75.  
<https://doi.org/10.1007/s11707-012-0347-6>

Nag, S.K., Kundu, A. 2018. Application of Remote Sensing, GIS and MCA Techniques for Delineating Groundwater Prospect Zones in Kashipur Block, Purulia District, West Bengal. Applied Water Science, vol. 8, p. 1-13. <https://doi.org/10.1007/s13201-018-0679-9>

Nasir, M.J., Khan, S., Ayaz, T., Khan, A.Z., Ahmad, W., Lei, M. 2021. An Integrated Geospatial Multi-Influencing Factor Approach to Delineate and Identify Groundwater Potential Zones in Kabul Province, Afghanistan. Environmental Earth Sciences, v. 80(13), 453.  
<https://doi.org/10.1007/s12665-021-09742-z>

Nasir, M.J., Khan, S., Zahid, H., Khan, A. 2018. Delineation of Groundwater Potential Zones Using GIS and Multi Influence Factor (MIF) Techniques: A Study of District Swat, Khyber Pakhtunkhwa, Pakistan. Environmental Earth Sciences, v. 77, p. 1-11.  
<https://doi.org/10.1007/s12665-018-7522-3>

O'Leary, D.W., Friedman, J.D., Pohn, H.A. 1976. Lineament, Linear, Lineation: Some Proposed New Standards for Old Terms. Geological Society of America Bulletin,

vol. 87(10), p. 1463-1469. [https://doi.org/10.1130/0016-7606\(1976\)87<1463:LLSPN>2.0.CO;2](https://doi.org/10.1130/0016-7606(1976)87<1463:LLSPN>2.0.CO;2)

Oh, H.J., Kim, Y.S., Choi, J.K., Park, E., Lee, S. 2011. GIS Mapping of Regional Probabilistic Groundwater Potential in the Area of Pohang City, Korea. *Journal of Hydrology*, v. 399(3-4), p. 158-172. <https://doi.org/10.1016/j.jhydrol.2010.12.027>

Preeja, K.R., Joseph, S., Thomas, J., Vijith, H. 2011. Identification of Groundwater Potential Zones of a Tropical River Basin (Kerala, India) Using Remote Sensing and GIS Techniques. *Journal of the Indian Society of Remote Sensing*, v. 39, p. 83-94. <https://doi.org/10.1007/s12524-011-0075-5>

Qureshi, A.S. 2015. Improving Food Security and Livelihood Resilience through Groundwater Management in Pakistan. *Global Advanced Research Journal of Agricultural Science*, v. 4, p. 687-710

Rahman, K.U., Shang, S., Zohaib, M. 2021. Assessment of Merged Satellite Precipitation Datasets in Monitoring Meteorological Drought over Pakistan. *Remote Sensing*, vol. 13(9), p. 1662. <https://doi.org/10.3390/rs13091662>

Rajasekhar, M., Gadhira, S.R., Kadam, A., Bhagat, V. 2020. Identification of Groundwater Recharge-Based Potential Rainwater Harvesting Sites for Sustainable Development of a Semiarid Region of Southern India Using Geospatial, AHP, and SCS-CN Approach. *Arabian Journal of Geosciences*, v. 13(2), 24. <https://doi.org/10.1007/s12517-019-4996-6>

Ramu, Mahalingam, B., Vinay, M. 2015. Identification of Groundwater Potential Zones Using GIS and Remote Sensing Techniques: A Case Study of Mysore Taluk-Karnataka. *International Journal of Geomatics and Geosciences*, v. 5(3), p. 393-403.

Saravanan, S., Saranya, T., Abijith, D. 2022. Application of Frequency Ratio, Analytical Hierarchy Process, and Multi-Influencing Factor Methods for Delineating Groundwater Potential Zones. *International Journal of Environmental Science and Technology*, v. 19(12), p. 12211-12234.

<https://doi.org/10.1007/s13762-021-03794-1>

Sato, H., Shibusaki, N., Van Lap, N., Oanh, T.T.K., Lan, N.T.M. 2019. Characteristics on Distribution of Chemical Composition in Groundwater along the Mekong and Bassac (Hậu) River, Vietnam. *Vietnam Journal of Earth Sciences*, v. 41(3), p. 272-288. <https://doi.org/10.15625/0866-7187/41/3/13969>

Selvam, S., Magesh, N.S., Chidambaram, S., Rajamanickam, M., Sashikkumar, M.C. 2015. A GIS Based Identification of Groundwater Recharge Potential Zones Using RS and IF Technique: A Case Study in Ottapidaram Taluk, Tuticorin District, Tamil Nadu. *Environmental Earth Sciences*, vol. 73, p. 3785-3799. <https://doi.org/10.1007/s12665-014-3664-0>

Senanayake, I.P., Dissanayake, D.M.D.O.K., Mayadunna, B.B., Weerasekera, W.L. 2016. An Approach to Delineate Groundwater Recharge Potential Sites in Ambalantota, Sri Lanka Using GIS Techniques. *Geoscience Frontiers*, v. 7(1), p. 115-124. <https://doi.org/10.1016/j.gsf.2015.03.002>

Shao, Z., Huq, M. E., Cai, B., Altan, O., Li, Y. 2020. Integrated remote sensing and GIS approach using Fuzzy-AHP to delineate and identify groundwater potential zones in semi-arid Shanxi Province, China. *Environmental Modelling & Software*, vol. 134, 104868. <https://doi.org/10.1016/j.envsoft.2020.104868>

Shinde, S.P., Barai, V.N., Gavit, B.K., Kadam, S.A., Atre, A.A., Pande, C.B., Pal, S.C., Radwan, N., Tolche, A.D., Elkhrahy, I. 2024. Assessment of groundwater potential zone mapping for semi-arid environment areas using AHP and MIF techniques. *Environmental Sciences Europe*, 36(1), 87. <https://doi.org/10.1186/s12302-024-00906-9>

Sohail, A.T., Singh, S.K., Kanga, S. 2019. A Geospatial Approach for Groundwater Potential Assessment Using Multi Influence Factor (MIF) Technique. *International Journal on Emerging Technologies*, vol. 10(1), p. 183-196.

Strahler, A.N. 1964. Quantitative geomorphology of drainage basins and channel networks. In: Chow, V.T. (ed.), *Handbook of Applied Hydrology*, McGraw

Hill, New York, 439-476.

Tachikawa, T., Hato, M., Kaku, M., Iwasaki, A. 2011. Characteristics of ASTER GDEM version 2. 2011 IEEE International Geoscience and Remote Sensing Symposium, p. 3657-3660.  
<https://doi.org/10.1109/IGARSS.2011.6050017>

Tailor, D., Shrimali, N.J. 2016. Surface runoff estimation by SCS curve number method using GIS for Rupen-Khan watershed, Mehsana district, Gujarat. Journal of the Indian Water Resources Society, vol. 36(4), p. 1-5

Thapa, R., Gupta, S., Guin, S., Kaur, H. 2017. Assessment of groundwater potential zones using multi-influencing factor (MIF) and GIS: A case study from Birbhum district, West Bengal. Applied Water Science, vol. 7, p. 4117-4131.  
<https://doi.org/10.1007/s13201-017-0571-z>

Trung, D.T., Nhan, N.T., Don, T.V., Hung, N.K., Kazmierczak, J., Nhan, P.Q. 2020. The Controlling of Paleo-Riverbed Migration on Arsenic Mobilization in Groundwater in the Red River Delta, Vietnam. Vietnam Journal of Earth Sciences, v. 42(2), p. 161-175.  
<https://doi.org/10.15625/0866-7187/42/2/14998>

USGS 2025. <https://www.usgs.gov/centers/eros/science/usgs-eros-archive-sentinel-2> (Accessed 15 January 2022)

Vasanthavigar, M., Srinivasamoorthy, K., Prasanna, M.V. 2013. Identification of Groundwater Contamination Zones and Its Sources by Using Multivariate Statistical Approach in Thirumanimuthar Sub-Basin, Tamil Nadu, India. Environmental Earth Sciences, v. 68, p. 1783-1795.  
<https://doi.org/10.1007/s12665-012-1868-8>

Yadav, B., Malav, L.C., Jangir, A., Kharia, S.K., Singh, S.V., Yeasin, M., Yadav, K.K. 2023. Application of Analytical Hierarchical Process, Multi-Influencing Factor, and Geospatial Techniques for Groundwater Potential Zonation in a Semi-Arid Region of Western India. Journal of Contaminant Hydrology, v. 253, 104122.  
<https://doi.org/10.1016/j.jconhyd.2022.104122>

Yin, J., Yin, Z., Zhong, H., Xu, S., Hu, X., Wang, J., Wu, J. 2011. Monitoring Urban Expansion and Land Use/Land Cover Changes of Shanghai Metropolitan Area During the Transitional Economy (1979-2009) in China. Environmental Monitoring and Assessment, vol. 177, p. 609-621. <https://doi.org/10.1007/s10661-010-1660-8>

Zghibi, A., Mirchi, A., Msaddek, M.H., Merzougui, A., Zouhri, L., Taupin, J.D., Tarhouni, J. 2020. Using Analytical Hierarchy Process and Multi-Influencing Factors to Map Groundwater Recharge Zones in a Semi-Arid Mediterranean Coastal Aquifer. Water, vol. 12(9), p. 2525.  
<https://doi.org/10.3390/w12092525>